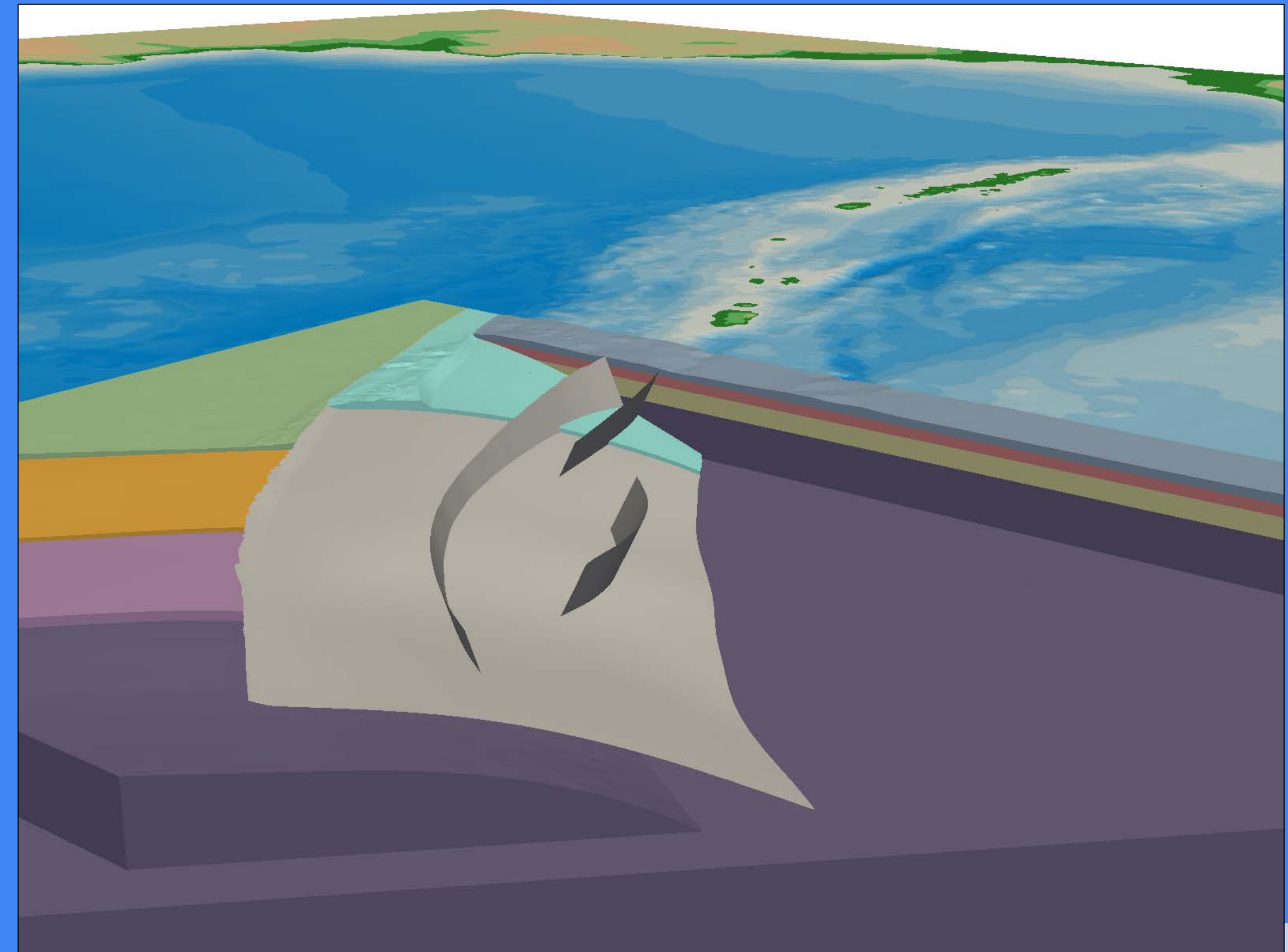


# Probing the state of pore fluid pressure and 3D megathrust earthquake dynamics using numerical models of the 2004 Sumatra-Andaman earthquake

- *Pore fluid pressure (Pf) may explain multiple observations of subduction zone megathrust behavior, but its coseismic state and influence on rupture dynamics are poorly constrained.*



**Elizabeth (Betsy) Madden**

**Thomas Ulrich**

**Alice-Agnes Gabriel**



**JGR Solid Earth** [betsymadden@gmail.com](mailto:betsymadden@gmail.com)

Research Article | [Open Access](#) | [CC BY](#)

**The State of Pore Fluid Pressure and 3-D Megathrust Earthquake Dynamics**

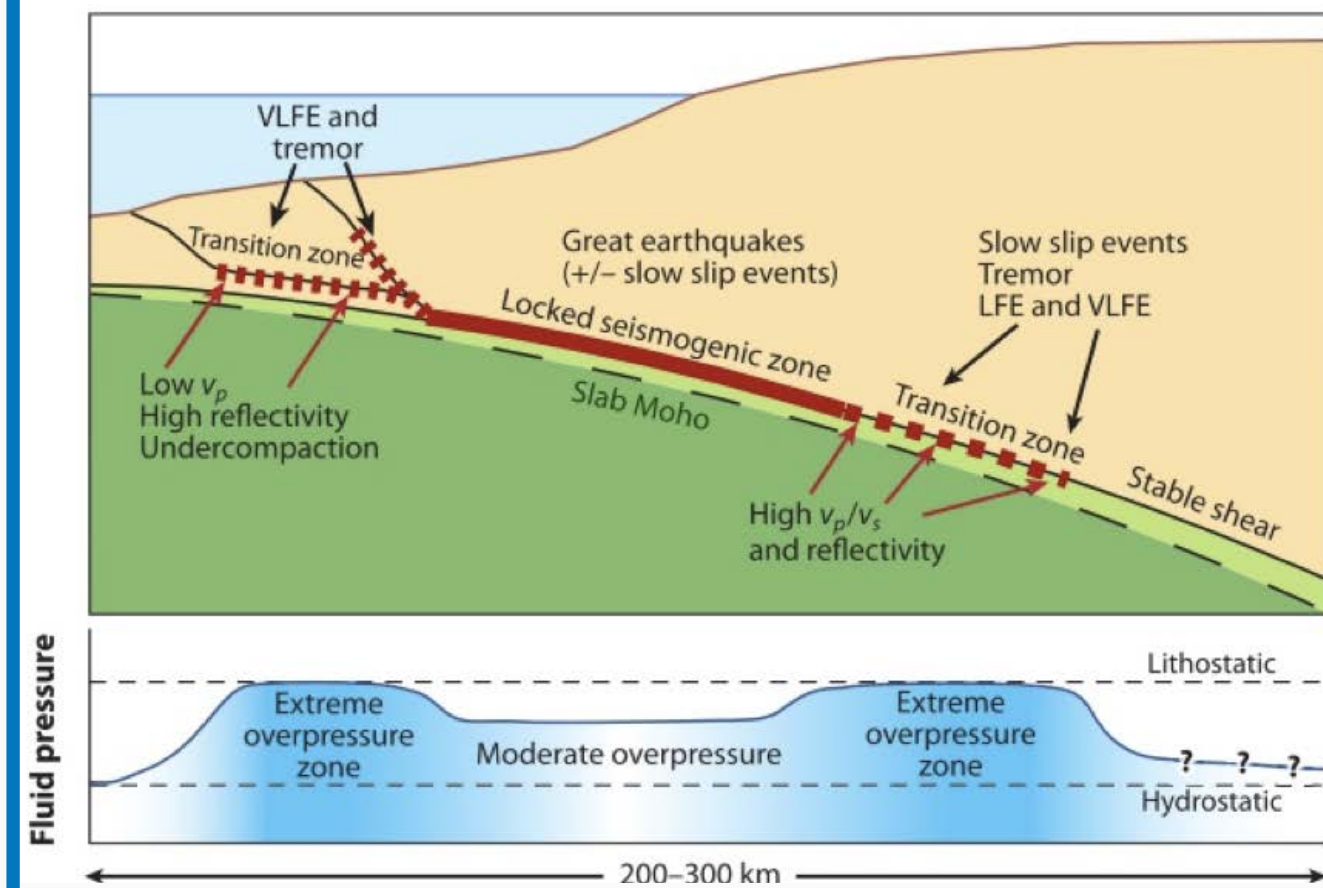
Elizabeth H. Madden Thomas Ulrich, Alice-Agnes Gabriel

First published: 16 March 2022 | <https://doi.org/10.1029/2021JB023382> | Citations: 1

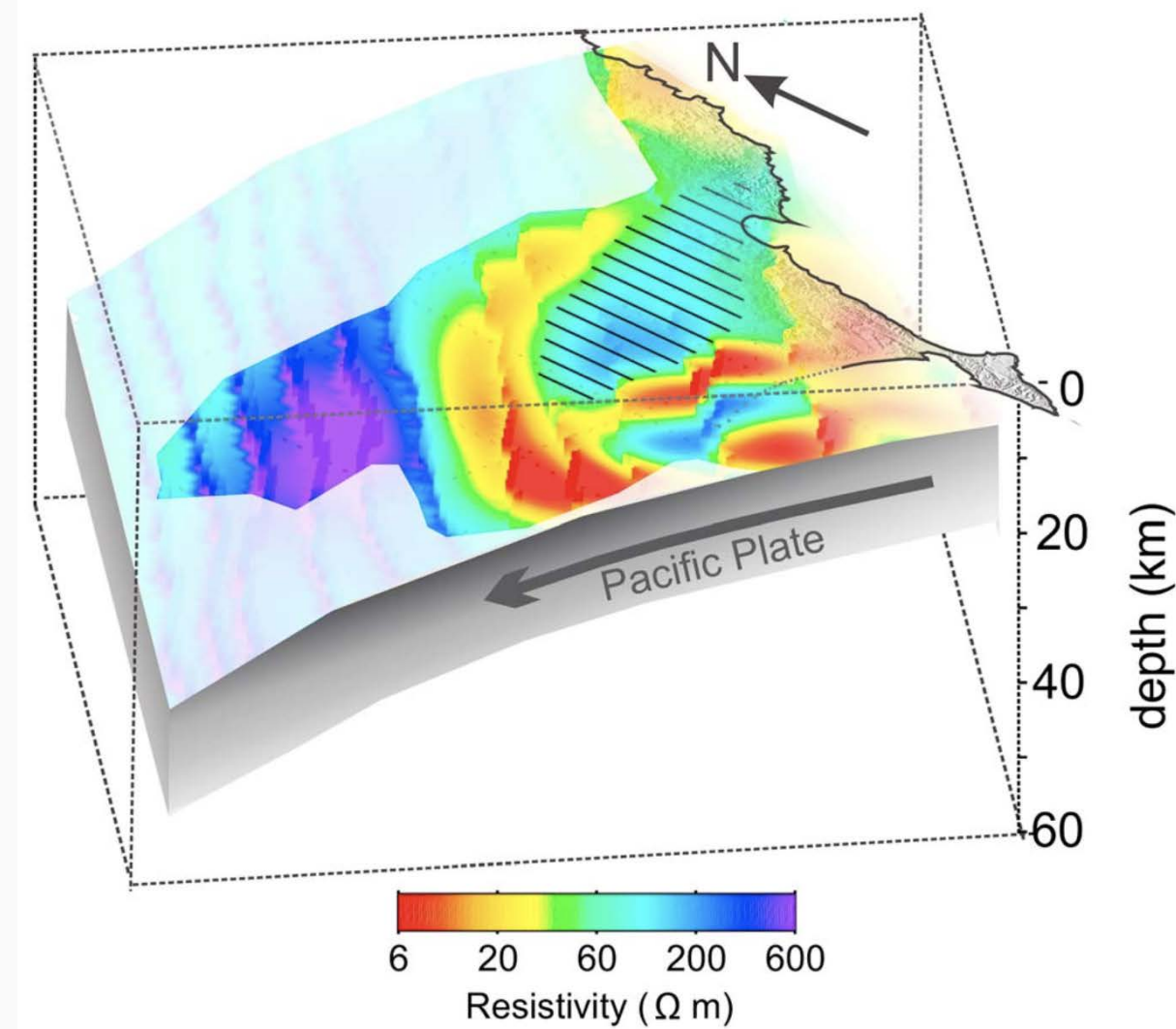
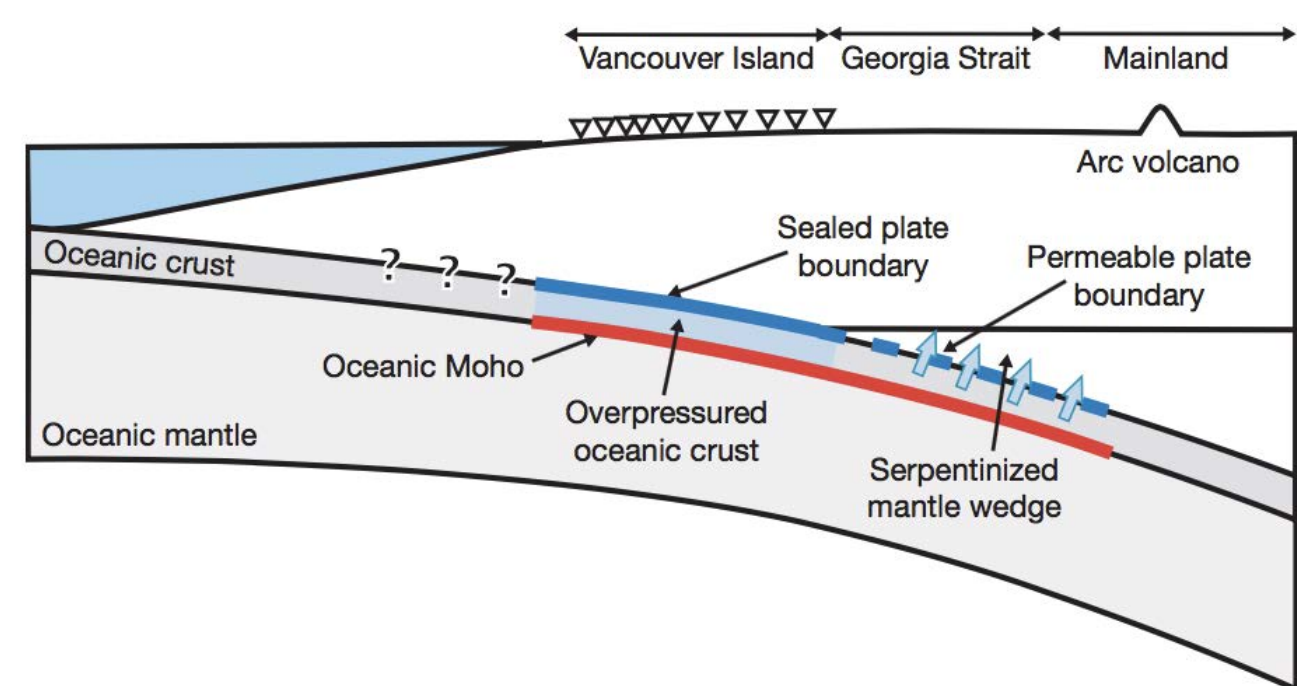
➤ What do we know about pore fluid pressure (Pf) along seismogenic portions of megathrusts?

- Interseismic period:  
Pf low to moderate  
Pf high in down-going plate
- Postseismic period:  
Pf is lithostatic
- Megathrust serves as barrier

**Interseismic Pf is elevated above hydrostatic along the locked megathrust that slips in big earthquakes and approaches lithostatic where "other" slip behavior is observed (Saffer & Tobin, 2011)**



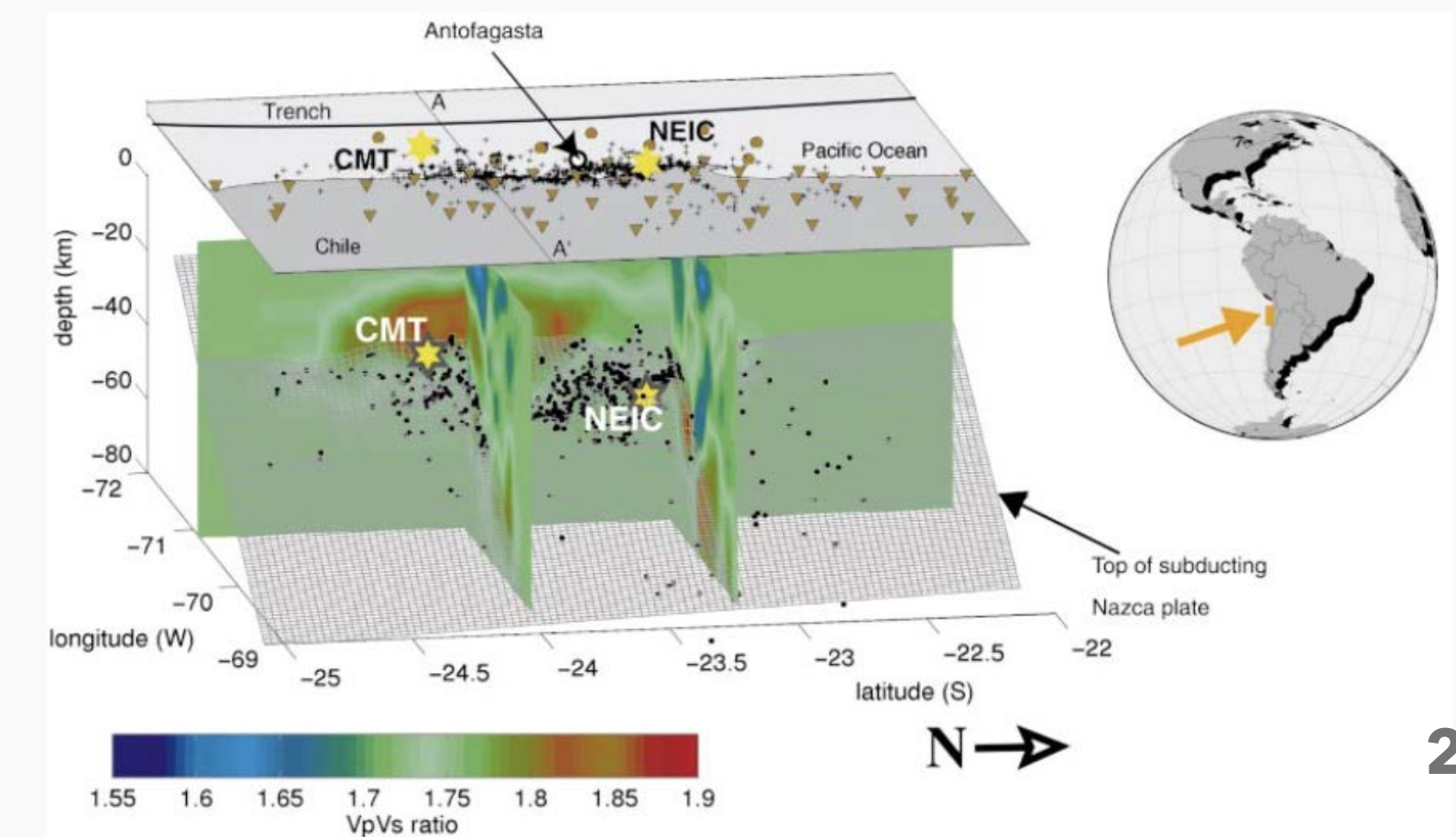
**Cascadia: High  $V_p/V_s$  ratio observed from receiver functions used to determine Poisson's ratio. Extrapolation of observed relationship between Poisson's ratio and Pf to 20-40km depth suggests **interseismic Pf in oceanic crust is lithostatic** (Audet et al., 2009)**



**Hikurangi: High resistivity patch is co-located with a geodetically identified coupled region. High resistivity indicates lack of fluid or low Pf, suggesting **low interseismic Pf**. (Heise et al., 2017)**

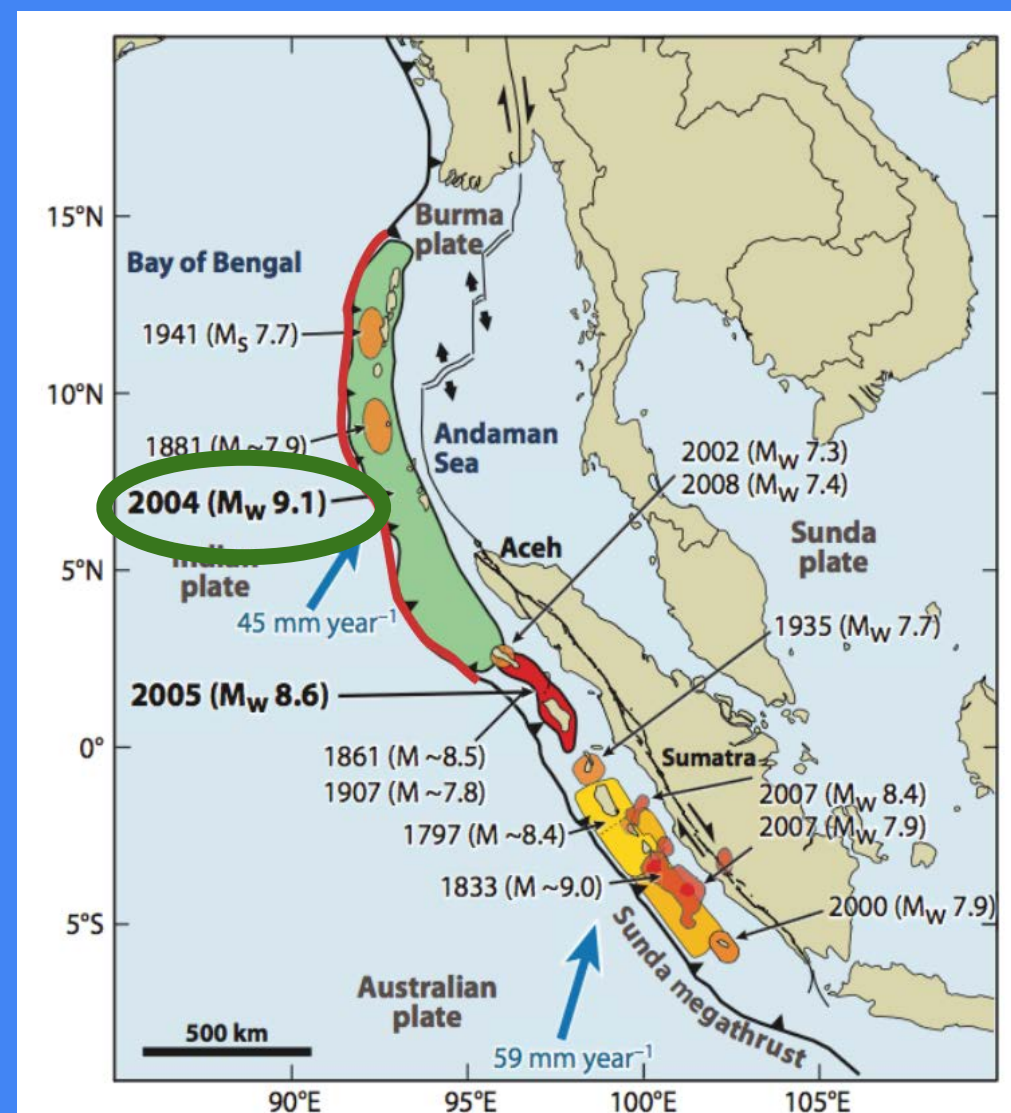
**Chile: Increases in  $V_p/V_s$  increases observed after 1995 M 8 Antofagasta earthquake (Husen & Kissling, 2001)**

- **Interseismic: high Pf in down-going plate**
- **Postseismic: high Pf in overriding plate as  $V_s$  decreases due to arriving fluids forcing cracks open**



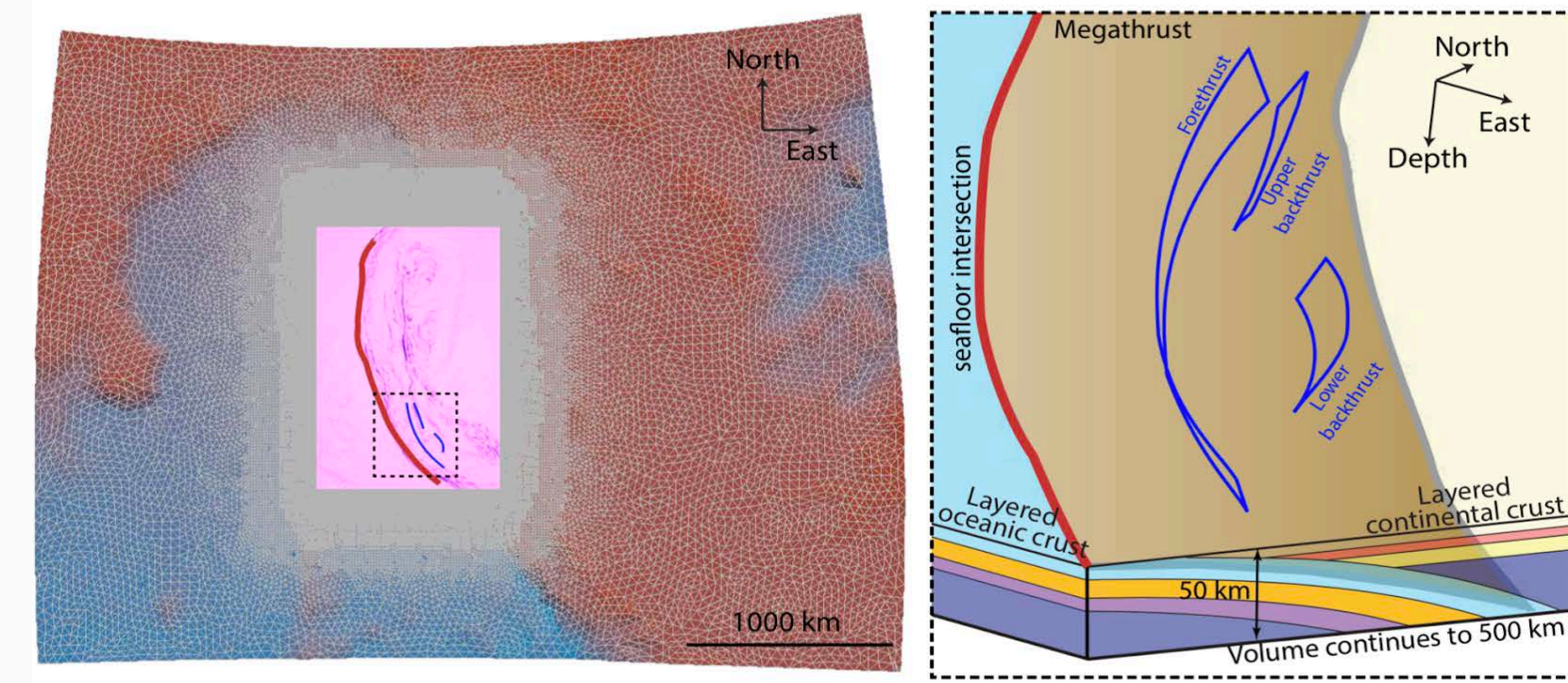
# But what happens coseismically?

We explore the influence of ***Pf*** on fault mechanics and first-order rupture dynamics using models based on the 2004 Mw 9.1 Sumatra-Andaman earthquake.



Shearer & Burgmann, 2010

Models are run with SeisSol, an open-source, 3D dynamic rupture & seismic wave propagation code optimized for high-performance computing (<https://github.com/SeisSol/SeisSol>, [www.seissol.org](http://www.seissol.org))



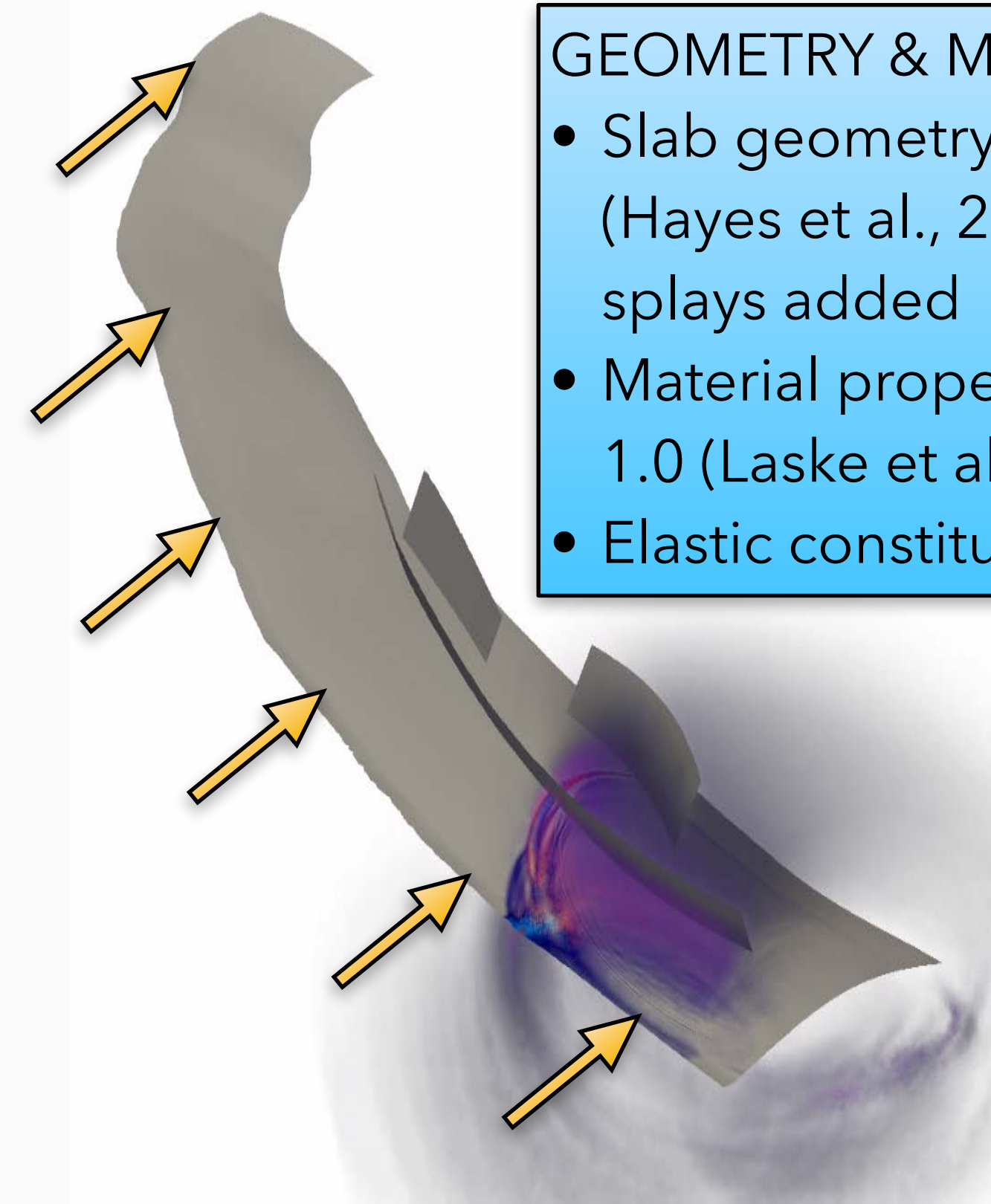
Uphoff et al (2017)

## STRESS ORIENTATION

- Uniform 3D stress field
- Maximum compressive stress at azimuth = 225°, plunge = 7° (focal mechanism inversion by Karagianni et al., 2016)

## FRICTIONAL PARAMETERS:

- Friction coefficients:  $\mu_s = 0.4, \mu_d = 0.1$
- Slip weakening distance:  $D_c = 0.8$  m
- On-fault cohesion:  $C = 0.4$  MPa, increases to 10 MPa at surface



## GEOMETRY & MATERIALS

- Slab geometry from Slab 1.0 (Hayes et al., 2012), with 3 splays added
- Material properties from Crust 1.0 (Laske et al., 2013)
- Elastic constitutive law

Slip and seismic waves from a SeisSol model of the 2004 Sumatra-Andaman earthquake under uniform remote loading.

# Model set-up: Pf magnitude and gradient

- **Absolute stress constant across all 6 scenarios**
- **Effective stress gradients assigned relative to the effective vertical (or lithostatic) stress:  $\sigma_v' = \rho g z + P_f$**

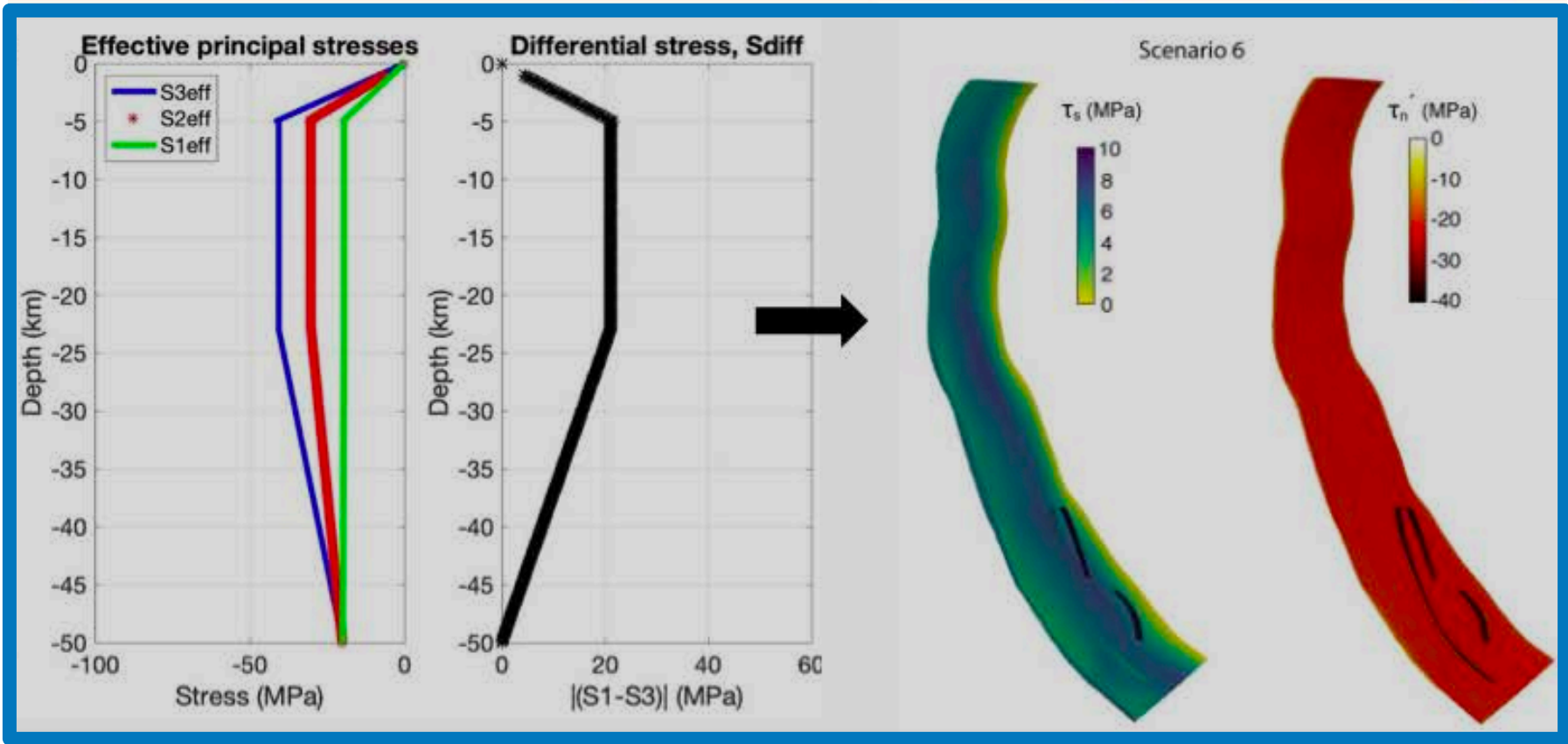
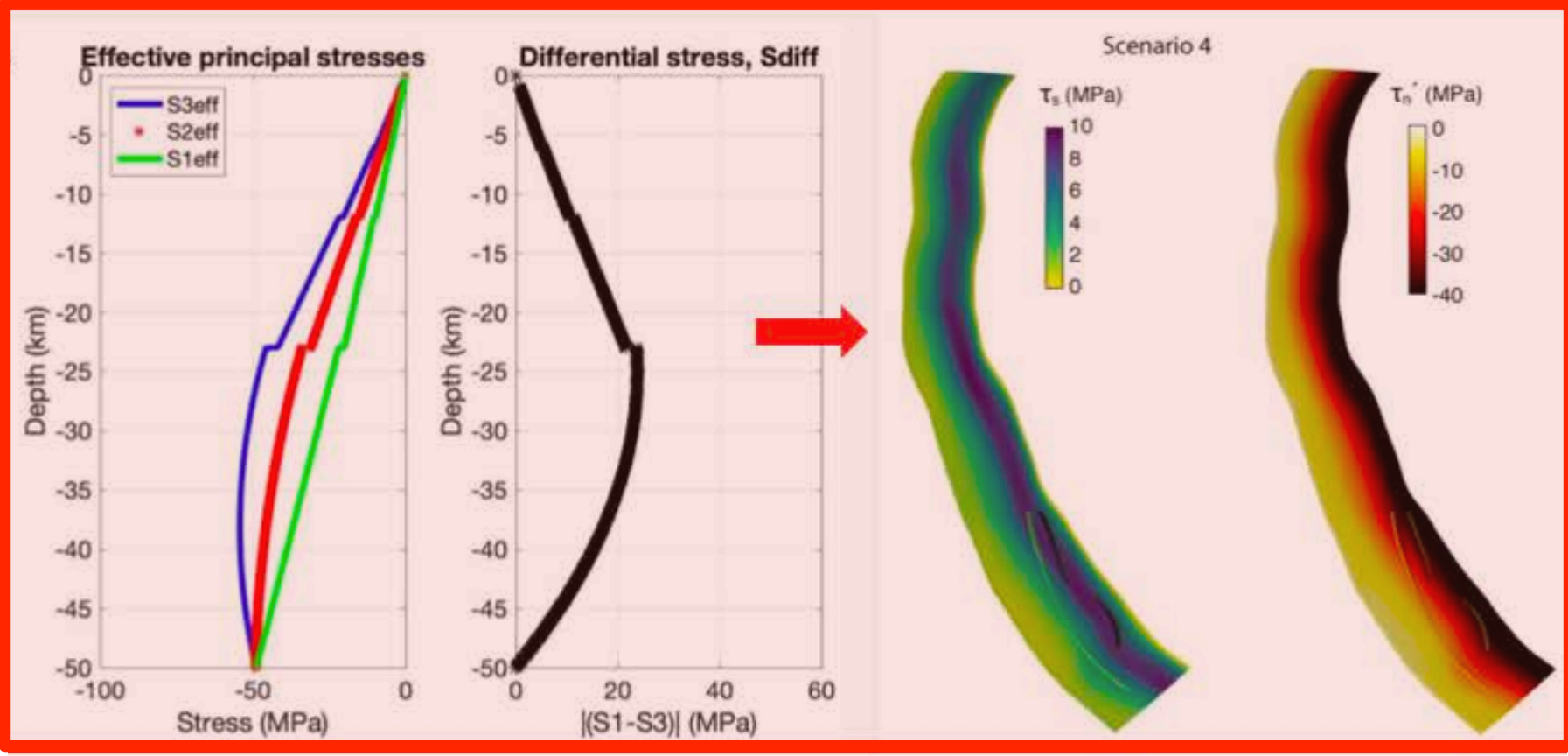
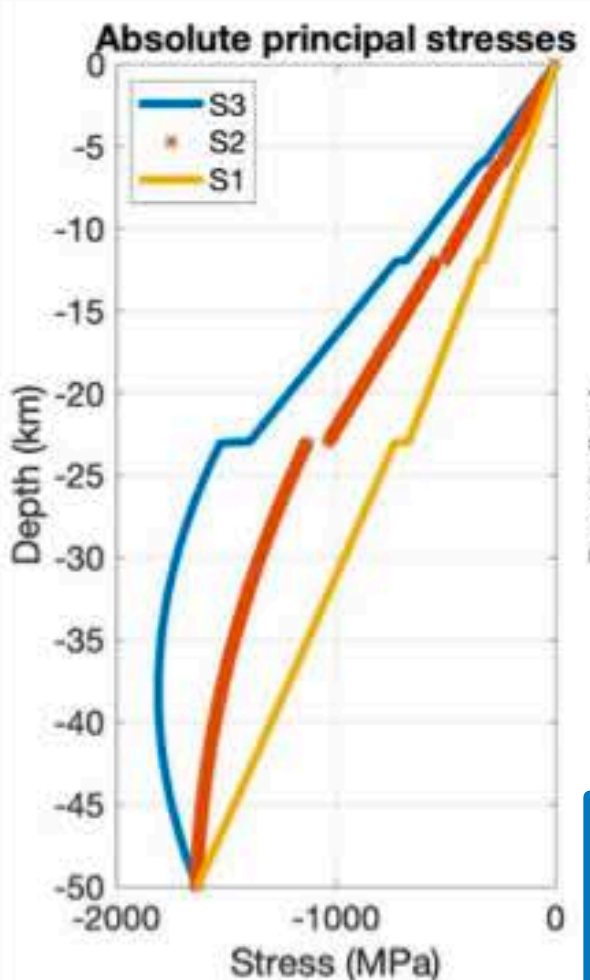
e.g. Hubbert and Rubey, 1959; Brace and Kohlstedt, 1989; Hirth and Beeler, 2015; Beeler et al., 2016; Harris et al., 2018

( $\rho$  = density of rock,  $g$  = gravitational acceleration,  $z$  = depth,  $P_f$  = pore fluid pressure)

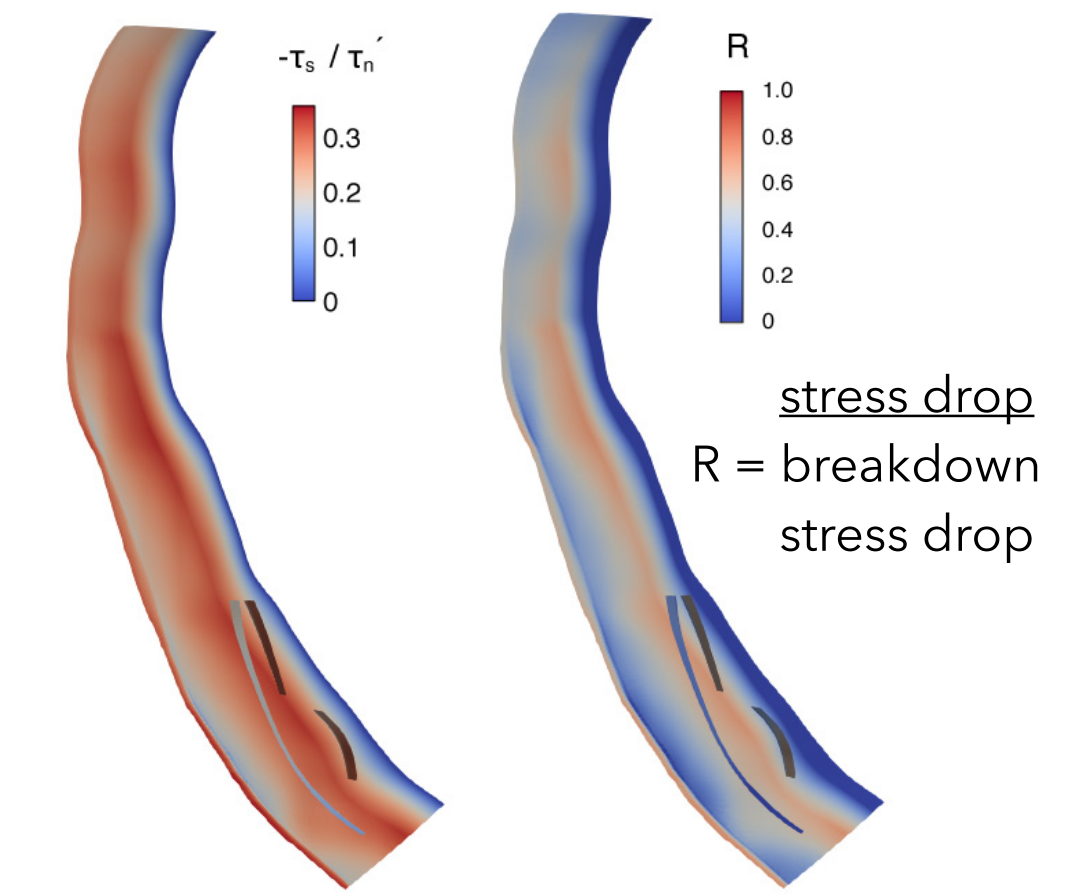
- **Scenarios 1 to 4: Sub-lithostatic Pf gradient leads to increasing normal stress with depth**

**Table 2**  
*Initial Conditions for All Scenarios*

Scenario	$P_f$ level (% of $\sigma_v^a$ )	$P_f$ parameterization
1	Low (31%)	$0.31\sigma_v$
2	Moderate (62%)	$0.62\sigma_v$
3	High (93%)	$0.93\sigma_v$
4	Very high (97%)	$0.97\sigma_v$
5	High (93%)	$\sigma_v - 42$ MPa
6	Very high (97%)	$\sigma_v - 20$ MPa



Ratio of shear to normal traction and R are constant across all models



- **Scenarios 5 and 6: Lithostatic Pf gradient leads to constant normal stress with depth**

e.g. Rice, 1992; Suppe, 2014

# Model results: Changing Pf magnitude

- Increase in Pf causes decreases in Mw, slip, peak slip rate, dynamic stress drop, rupture velocity
- Patterns of these parameters on megathrust do not change
- Scenarios 4 & 6 produce earthquake characteristics similar to observations: mean stress drop = 3 MPa (Seno, 2017), mean Vr = 2.4-2.6 km/s (Lay et al., 2005)

Pf

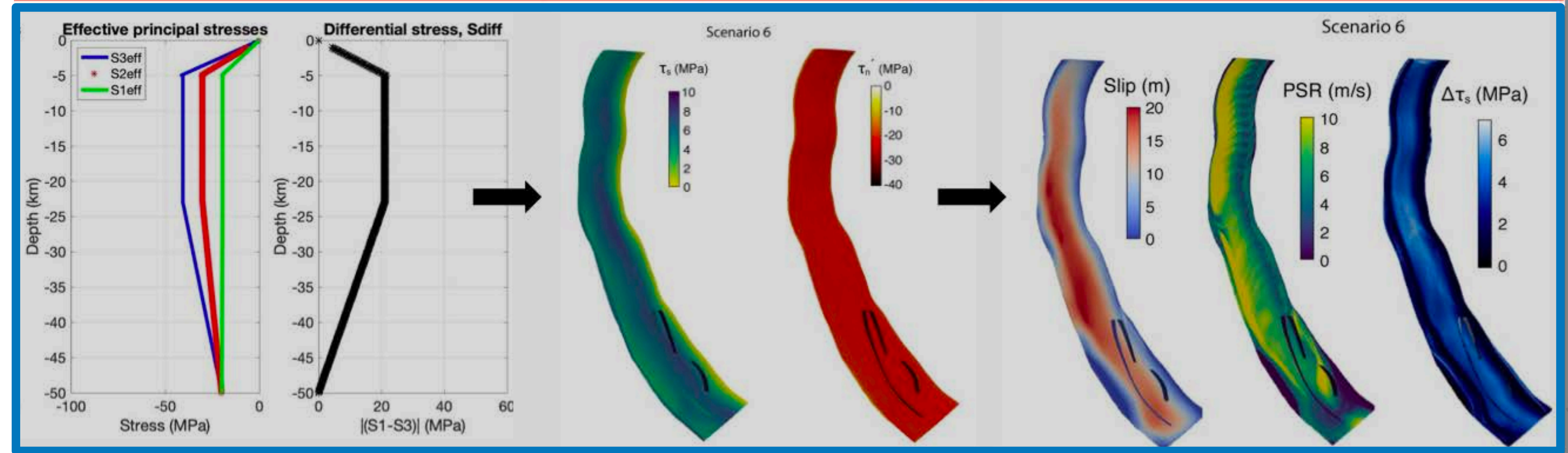
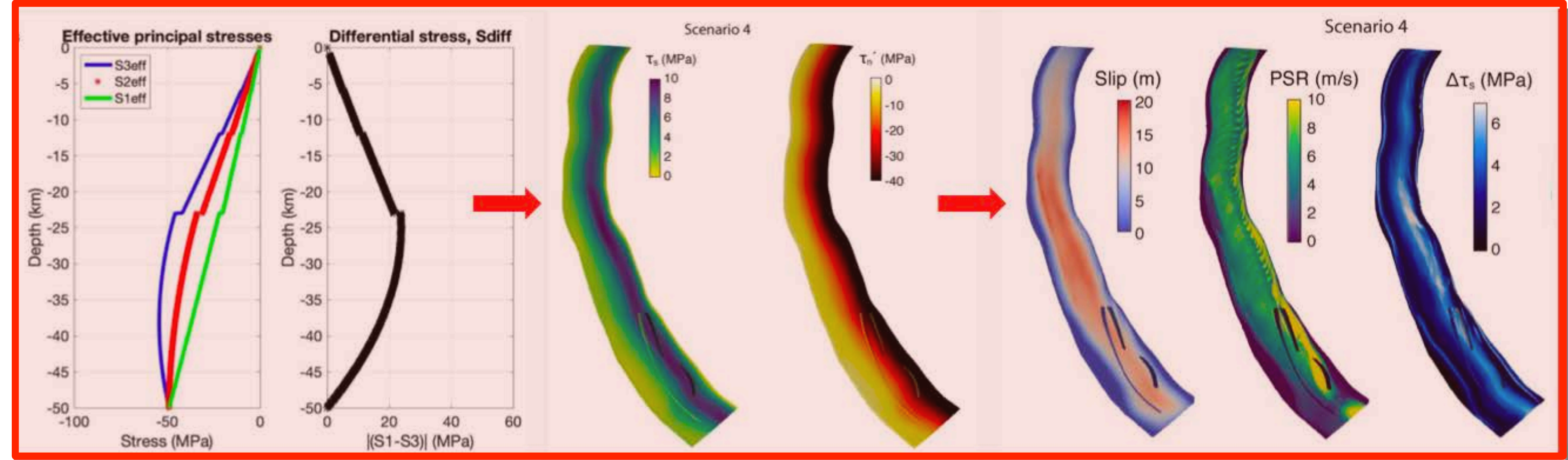
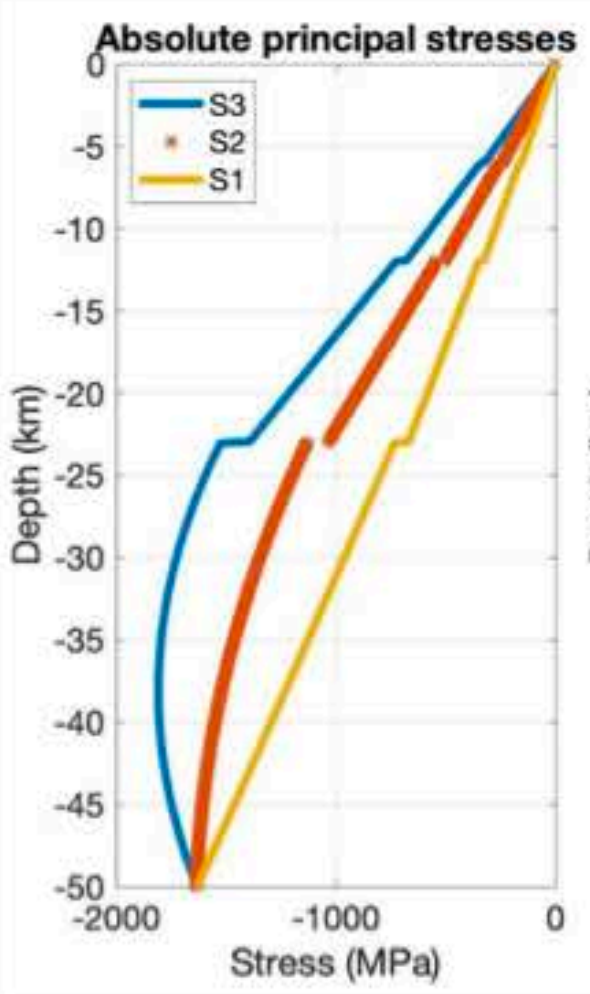
Table 3. Earthquake characteristics averaged across megathrust

Scen.	$M_w$	slip (m)	PSR (m/s) <sup>a</sup>	$\Delta\tau_s$ (MPa) <sup>b</sup>	$V_r$ (m/s) <sup>d</sup>
1	10.2	470	75	79	4765
2	9.9	235	46	42	4246
3	9.3	26	10	8	3025
4	9.0	8	5	3	2370
5	9.4	36	11	7	3203
6	9.1	10	6	3	2624

- Scenarios 1 to 4: Sub-lithostatic Pf gradient leads to increasing normal stress with depth

**Table 2**  
Initial Conditions for All Scenarios

Scenario	$P_f$ level (% of $\sigma_v$ ) <sup>a</sup>	$P_f$ parameterization
1	Low (31%)	$0.31\sigma_v$
2	Moderate (62%)	$0.62\sigma_v$
3	High (93%)	$0.93\sigma_v$
4	Very high (97%)	$0.97\sigma_v$
5	High (93%)	$\sigma_v - 42$ MPa
6	Very high (97%)	$\sigma_v - 20$ MPa



- Scenarios 5 and 6: Lithostatic Pf gradient leads to constant normal stress with depth e.g. Rice, 1992; Suppe, 2014

# Model results: Changing Pf gradient

A change from sub-lithostatic to lithostatic Pf gradient results in:

- Higher Mw, mean slip, mean rupture velocity
- Up-dip shift of peak slip and peak slip rate → increasing hazard
- Relatively constant stress drop across megathrust

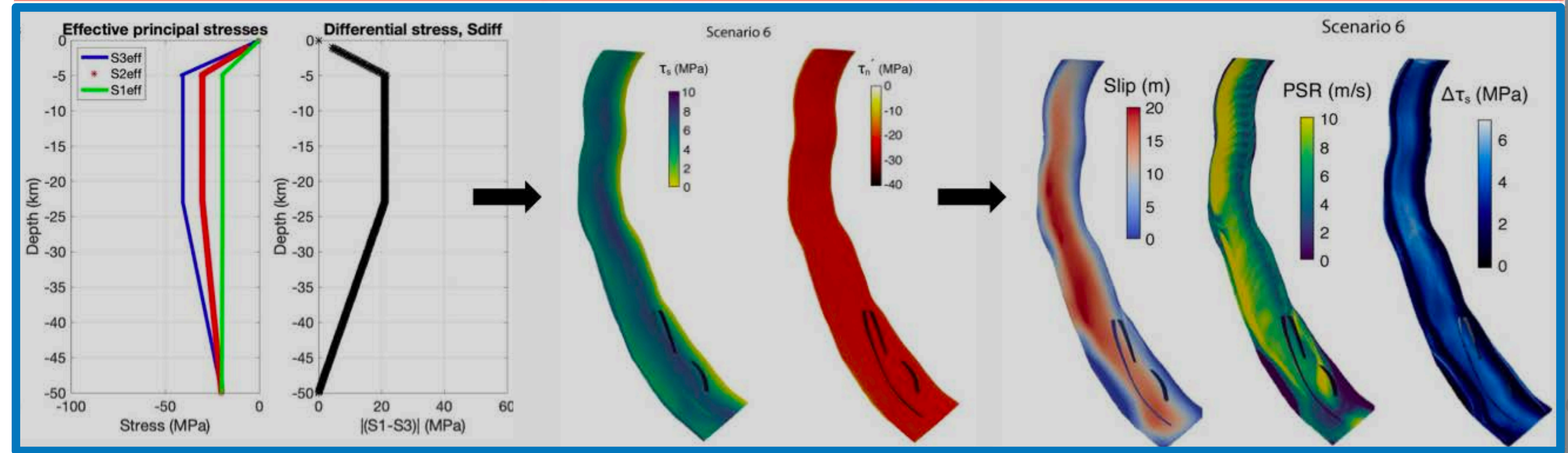
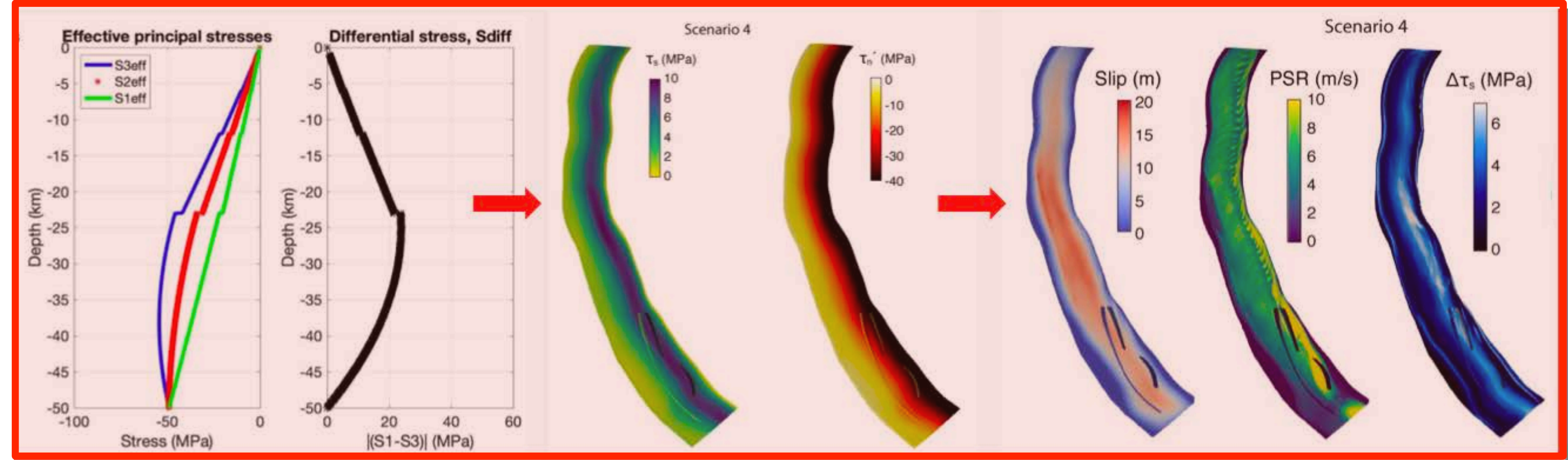
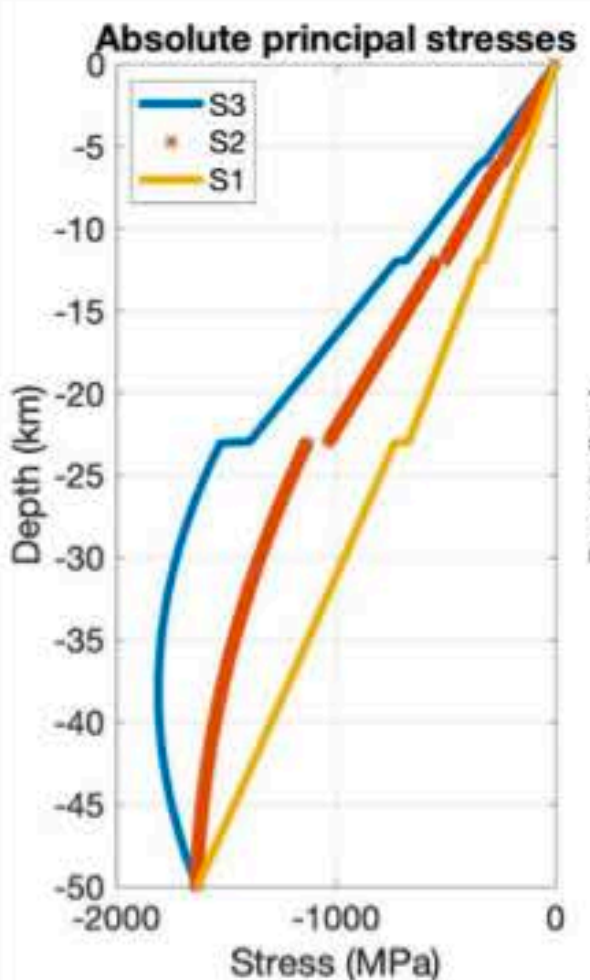
**Table 3.** Earthquake characteristics averaged across megathrust

Scen.	$M_w$	slip (m)	PSR (m/s) <sup>a</sup>	$\Delta\tau_s$ (MPa) <sup>b</sup>	$V_r$ (m/s) <sup>d</sup>
1	10.2	470	75	79	4765
2	9.9	235	46	42	4246
3	9.3	26	10	8	3025
4	9.0	8	5	3	2370
5	9.4	36	11	7	3203
6	9.1	10	6	3	2624

- **Scenarios 1 to 4: Sub-lithostatic Pf gradient leads to increasing normal stress with depth**

**Table 2**  
Initial Conditions for All Scenarios

Scenario	$P_f$ level (% of $\sigma_v$ ) <sup>a</sup>	$P_f$ parameterization
1	Low (31%)	$0.31\sigma_v$
2	Moderate (62%)	$0.62\sigma_v$
3	High (93%)	$0.93\sigma_v$
4	Very high (97%)	$0.97\sigma_v$
5	High (93%)	$\sigma_v - 42$ MPa
6	Very high (97%)	$\sigma_v - 20$ MPa



- **Scenarios 5 and 6: Lithostatic Pf gradient leads to constant normal stress with depth**  
e.g. Rice, 1992; Suppe, 2014

# What have we learned about earthquake physics from [models of] recent large earthquakes?

## Scenarios 4 and 6 produce earthquakes with characteristics similar to observations of 2004 Sumatra-Andaman earthquake:

- Mean stress drop = 3 MPa (Seno, 2017)
- Mean rupture velocity = 2.4-2.6 km/s (Lay et al., 2005)

### → Suggesting that:

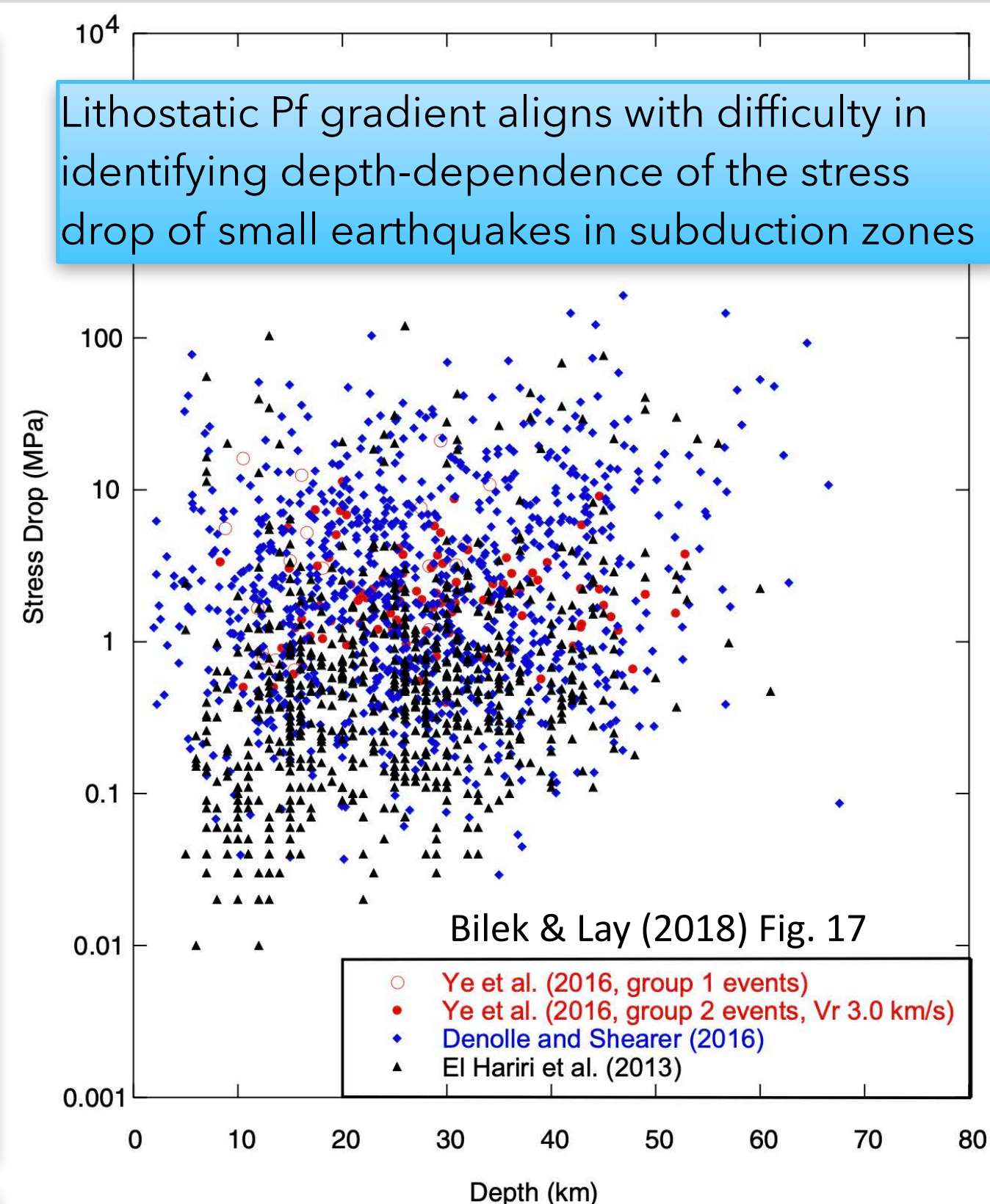
- **Pore fluid pressure is very high (~97 % of lithostatic load)**
- Mean shear traction is on the order of 4-5 MPa
- Mean effective normal traction is on the order of 22 MPa

### → Causing:

- Relatively low  $M_w$ , cumulative slip, peak slip rate, dynamic stress drop and rupture velocity on megathrust

## Changing from a **sub-lithostatic Pf gradient** leading to **increasing normal stress with depth** to a **lithostatic Pf gradient** leading to **constant normal stress with depth** causes:

- Higher  $M_w$ , mean slip, mean rupture velocity
- **Up-dip shift of peak slip and peak slip rate**
- **Relatively constant stress drop across megathrust**



- **A lithostatic Pf gradient should be considered in any determination of coseismic static frictional fault strength at depth.**
- **Conditions and constitutive behavior of near-trench materials must be constrained, as peak slip is shifted up-dip under a lithostatic Pf gradient.**

- Scenarios likely represent variable conditions present along a single megathrust due to spatial variations in Pf magnitude and/or gradient
- Scenarios also may represent variations that occur in time along megathrust
- Now time to layer back on complexities: **JGR Solid Earth** [betsymadden@gmail.com](mailto:betsymadden@gmail.com)  
Research Article | [Open Access](#) | [CC](#) | [i](#)  
The State of Pore Fluid Pressure and 3-D Megathrust Earthquake Dynamics  
Elizabeth H. Madden [✉](#), Thomas Ulrich, Alice-Agnes Gabriel [✉](#)  
First published: 16 March 2022 | <https://doi.org/10.1029/2021JB023382> | Citations: 1

How do natural fault zone complexities manifest on rupture dynamics?

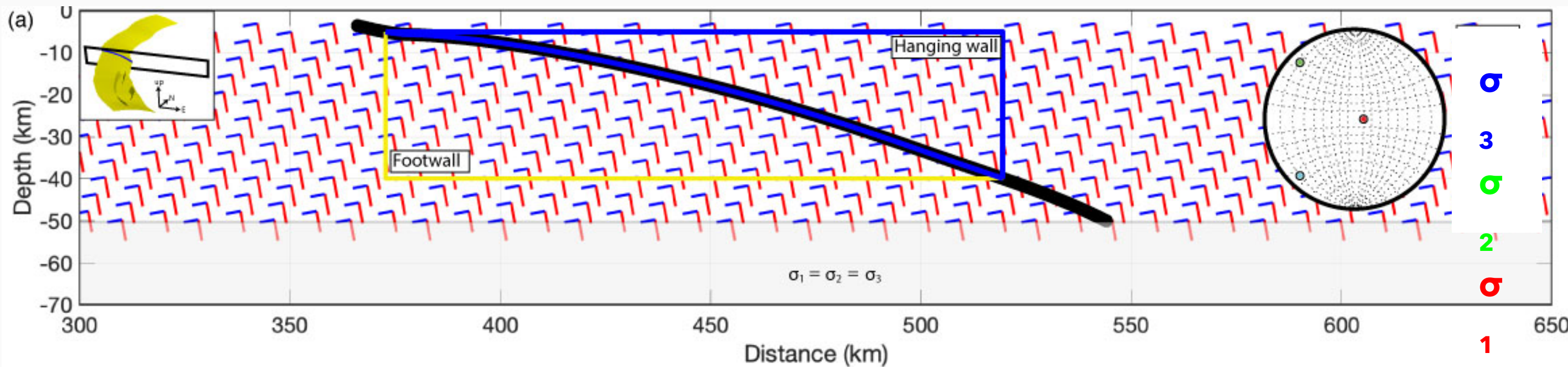
We invite all numerical, analytical, and experimental studies that address any of the above questions, with the purpose of developing a holistic understanding of the current challenges and future directions in -- deterministic, stochastic, and probabilistic -- joint studies of earthquake source physics and ground motion.

➤ Rotations are similar across all scenarios.

➤ Rotations are larger in the hanging wall than in the footwall.

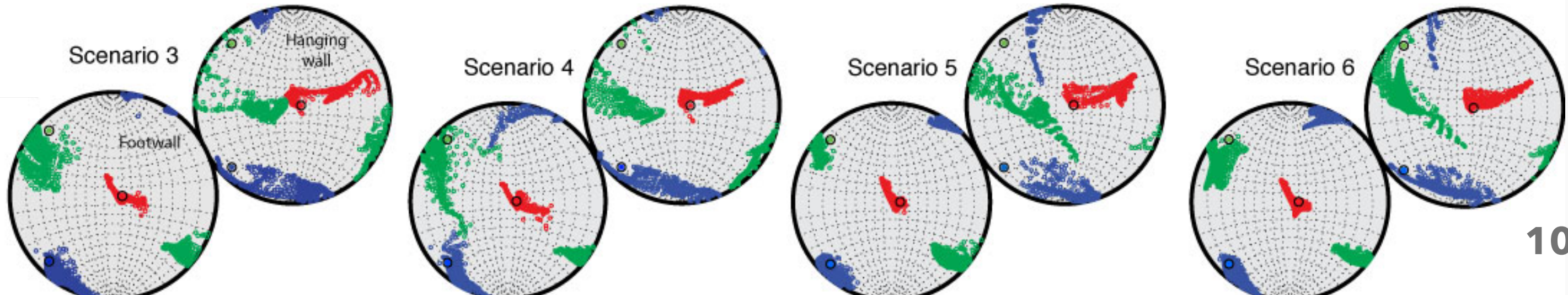
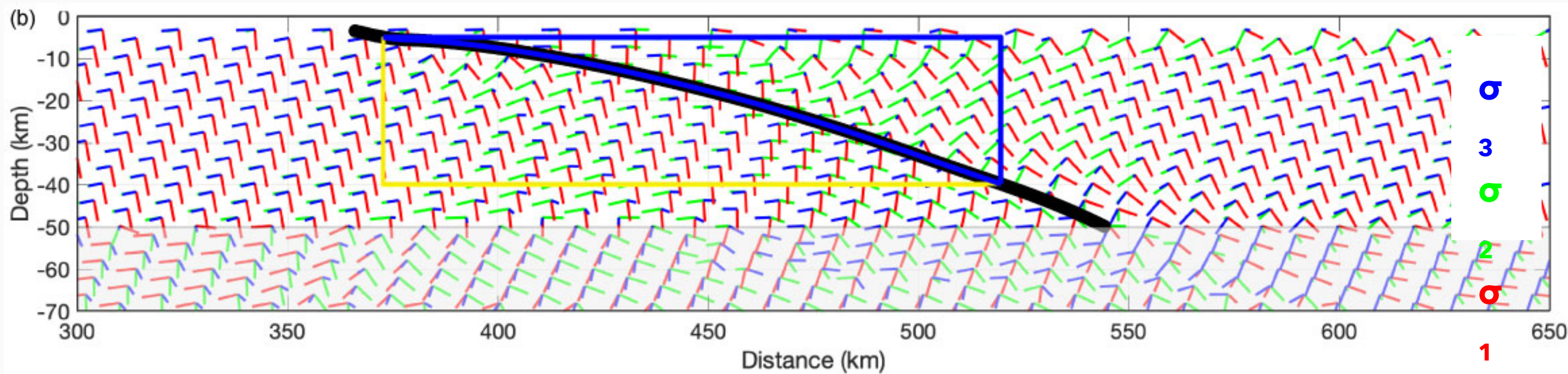
➤ Differential stress ( $|\sigma_3 - \sigma_1|$ ) in scenarios 4 and 6 is very low.

**Before the earthquake:**

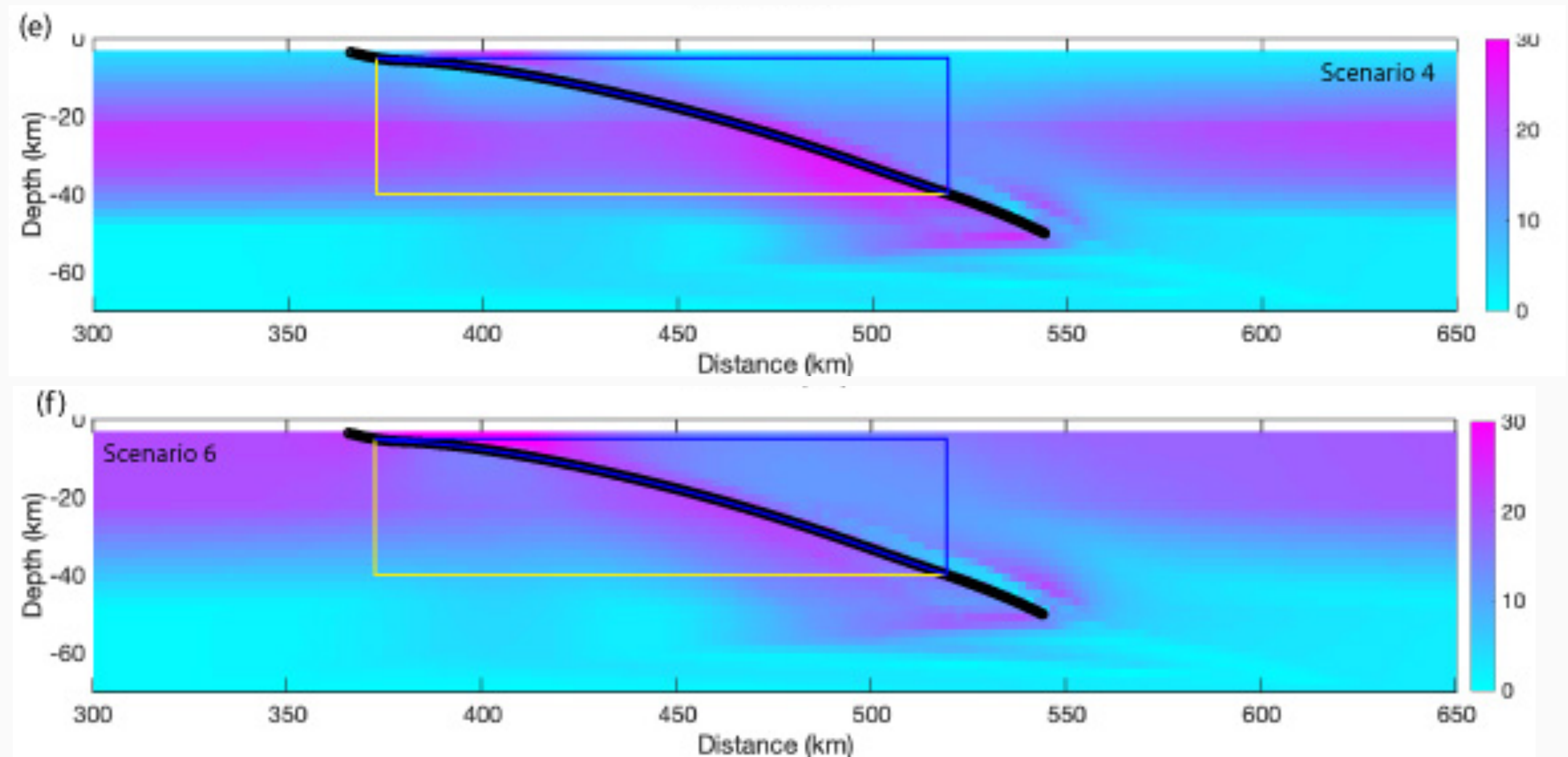


**After the earthquake:**

- **The maximum compressive stress,  $\sigma_3$ , rotates toward parallel with the trench, but does not change its plunge.**
- **$\sigma_2$  plunges more steeply.**
- **$\sigma_1$  plunges less steeply.**



- Rotations are similar across all scenarios.
- Rotations are larger in the hanging wall than in the footwall.
- Differential stress ( $\sigma_3 - \sigma_1$ ) in scenarios 4 and 6 is **very low**.



**This post-earthquake stress field is consistent with a variety of aftershock focal mechanisms, as is observed:**

- Of 125 Mw 5+ aftershocks with focal mechanisms solutions in the GCMT catalog occurring along the central rupture within 1 month of the mainshock:
  - **63 have strike-slip focal mechanisms**
  - **29 have reverse mechanisms**
  - **31 have normal mechanisms**
  - **2 cannot be categorized**

In summary, we have evaluated the role of ***Pf*** on subduction zone fault mechanics and earthquake dynamics with earthquake rupture models and found:

### GENERAL ***Pf*** EFFECTS:

- Increasing ***Pf*** decreases fault strength,  $M_w$ , cumulative slip, peak slip rate, stress drop, and rupture velocity.
- The preferred scenarios have **very high *Pf*** (97% of lithostatic load) and **very low mean shear** (4-5 MPa) and **effective normal tractions** (-22 MPa)...
- ...leading to **low mean stress drop** (3 MPa) and **low mean rupture velocity** (2.4-2.6 km/s).

### NORMAL STRESS CONDITIONS:

- Relative to a depth-dependent, constant normal stress moves peak slip and peak slip rate up-dip, and produces a more constant stress drop.
- For the same or a lower mean stress drop, constant normal stress leads to higher  $M_w$ , mean slip and mean rupture velocity.
- From these models alone, it is difficult to conclude the likelihood of either condition, and constant normal stress may be a localized condition...
- ...but this should be considered when estimating fault strength characteristics in subduction zones.

### POST-EARTHQUAKE STRESS FIELD

- Stress rotations are similar across all scenarios and are larger in the hanging wall than in the footwall.
- The post-earthquake stress field is consistent with a variety of aftershock focal mechanisms, as is observed.
- The differential stress in scenarios 4 and 6 is very low. In combination with a more heterogeneous initial stress field, a variety of aftershocks focal mechanisms is possible.

➤ We will first compare 4 scenarios with  **$P_f$**  ranging from hydrostatic to lithostatic and depth-dependent effective normal stress.

(Later, we will add 2 additional scenarios with constant normal stress.)

Scen.	$P_f$ level	$P_f^a$	mean $\sigma_{dev}^b$	mean $\sigma_m^c$
1	low	1000gz	115±103	-931±428
2	moderate	2200gz	61±54	-524±254
3	high	0.93ρgz	12±8	-94±42
4	very high	0.97ρgz	5±5	-40±18

Stress gradients are assigned relative to the effective vertical (or lithostatic) stress as:

$$\sigma_v' = \rho g z + P_f$$

$\rho$  = density of rock

$g$  = gravitational acceleration

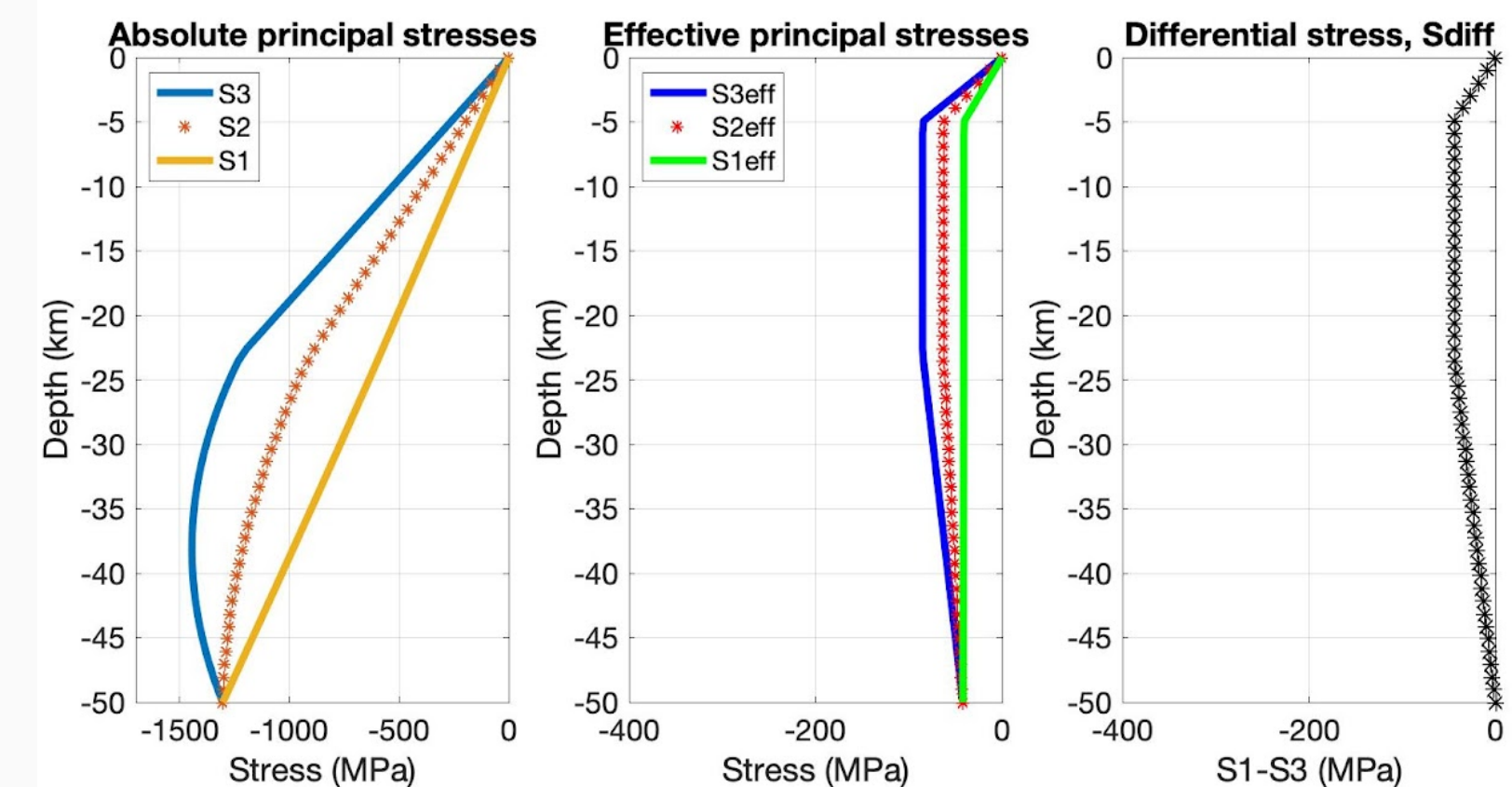
$z$  = depth

$P_f$  = pore fluid pressure

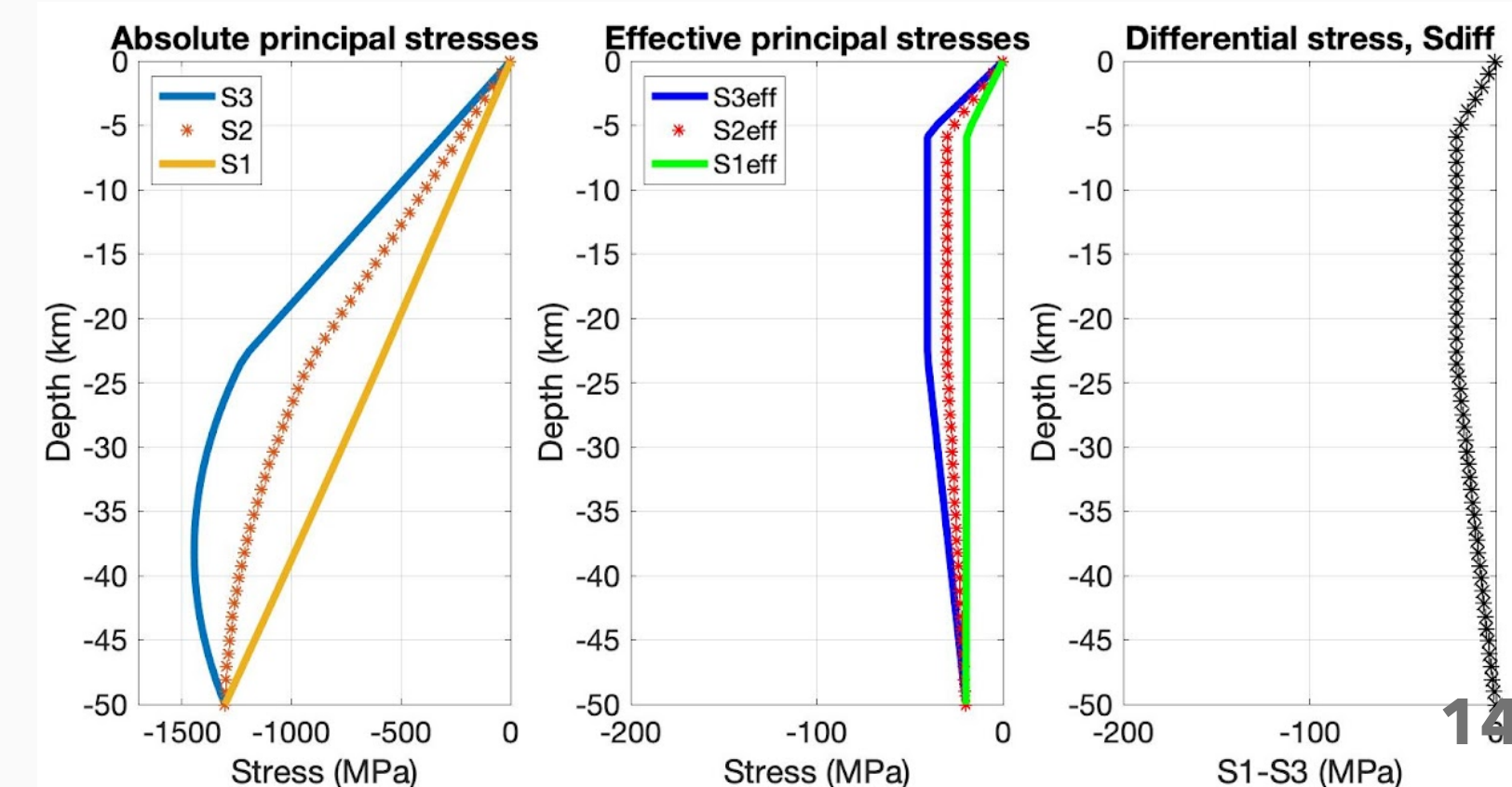
Thus, increasing  **$P_f$**  decreases:

- effective principal stress magnitudes,  $\sigma_3' < \sigma_2' < \sigma_1'$
- effective mean stress,  $\sigma_m'$
- effective deviatoric stress,  $\sigma_{dev}' = 0.5(\sigma_1' - \sigma_3')$ .

**Scenario 3: high  $P_f$**



**Scenario 4: very high  $P_f$**



➤ We will first compare 4 scenarios with fluid pressure ranging from hydrostatic to lithostatic and depth-dependent effective normal stress.

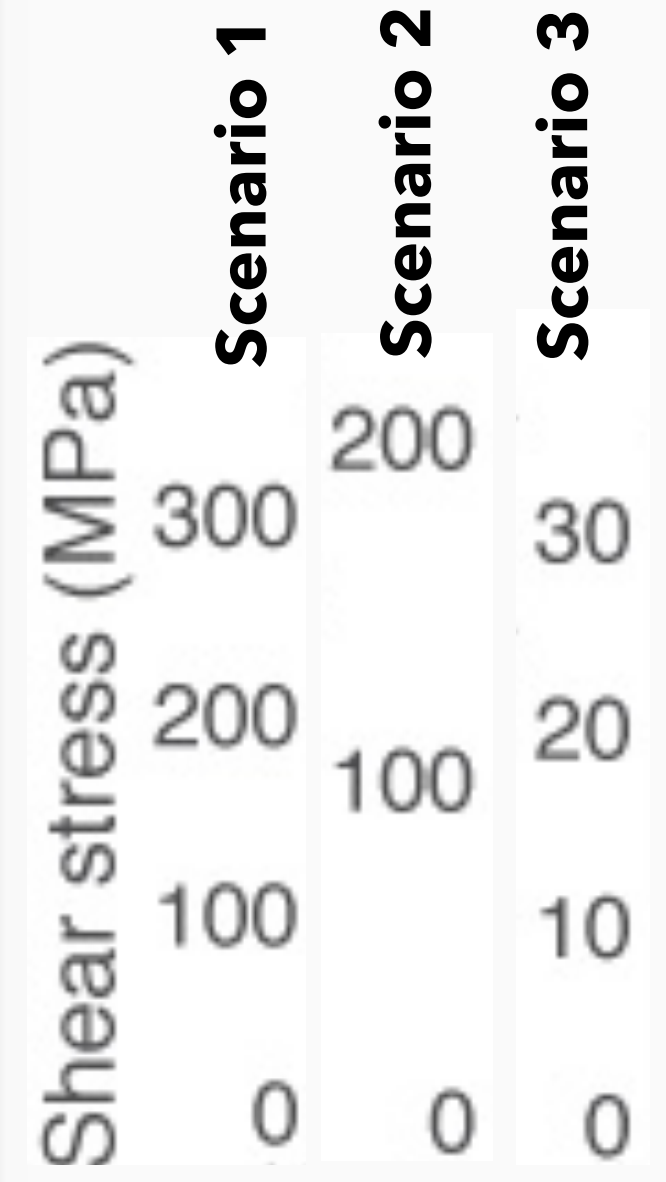
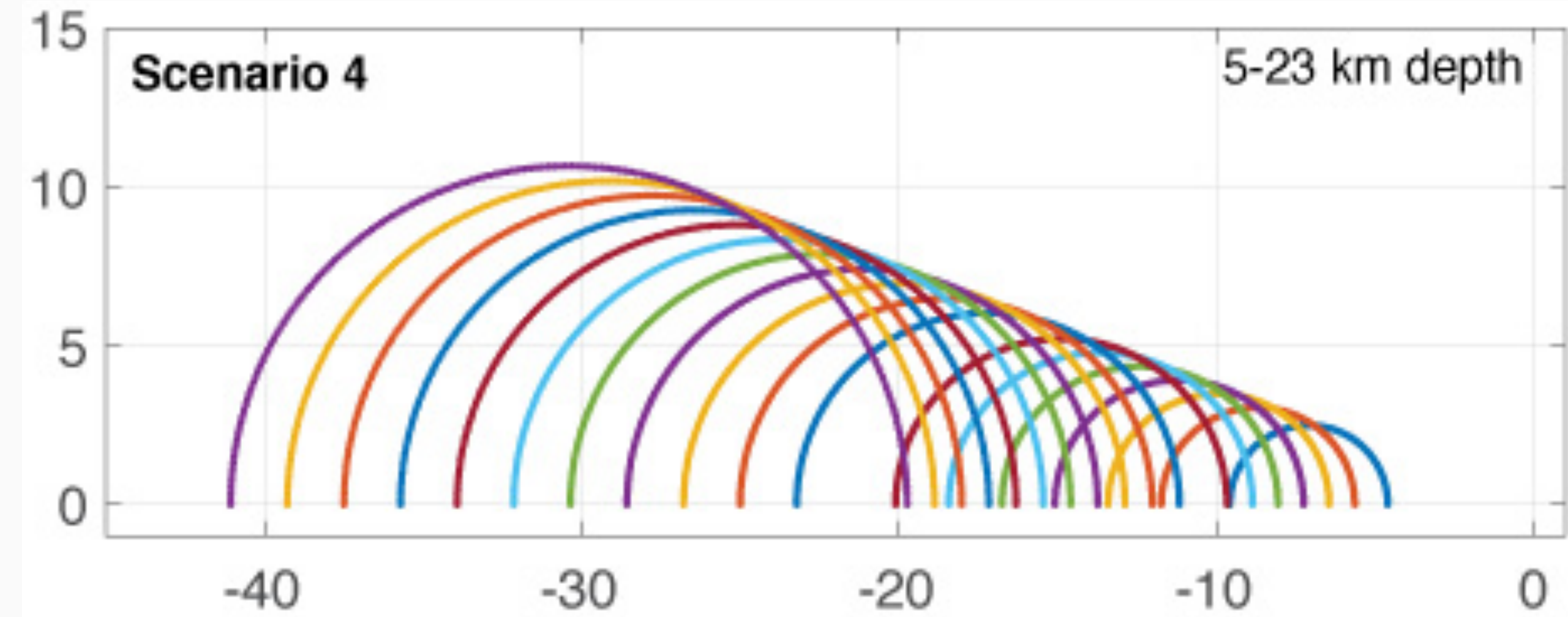
(Later, we will add 2 additional scenarios with constant normal stress.)

**Increasing  $P_f$ , decreasing shear traction**



Scen.	$P_f$ level	$P_f^a$	mean $\tau_o^d$	mean $\tau_n'^e$
1	low	$1000gz$	101	-506
2	moderate	$2200gz$	54	-277
3	high	$0.93\rho gz$	10	-52
4	very high	$0.97\rho gz$	4	-22

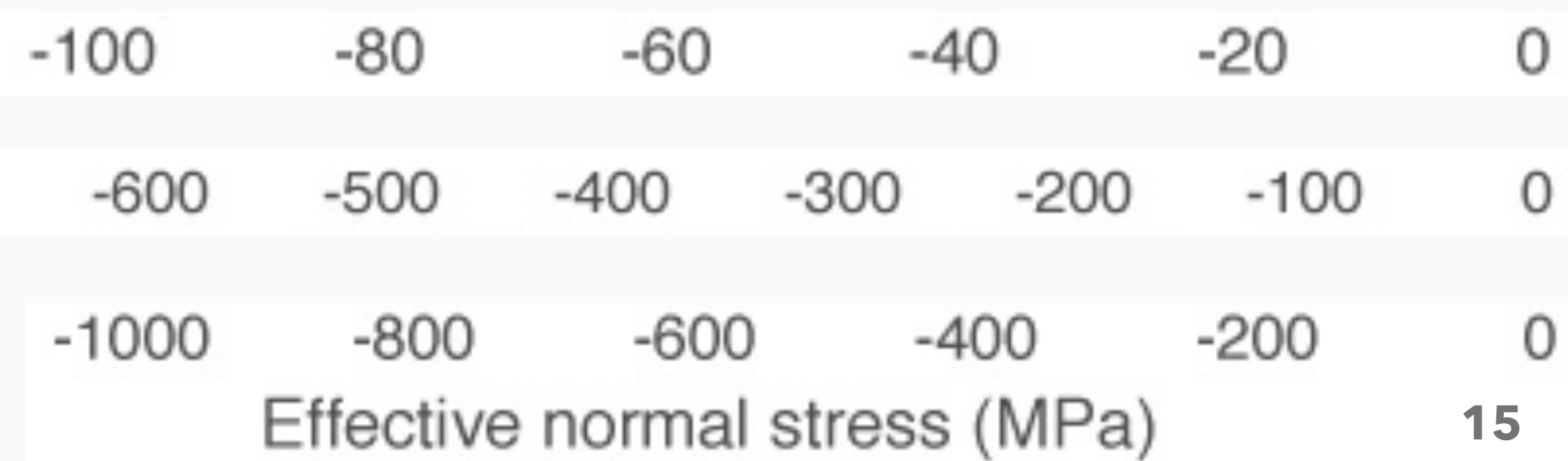
Scenario 1  
Scenario 2  
Scenario 3

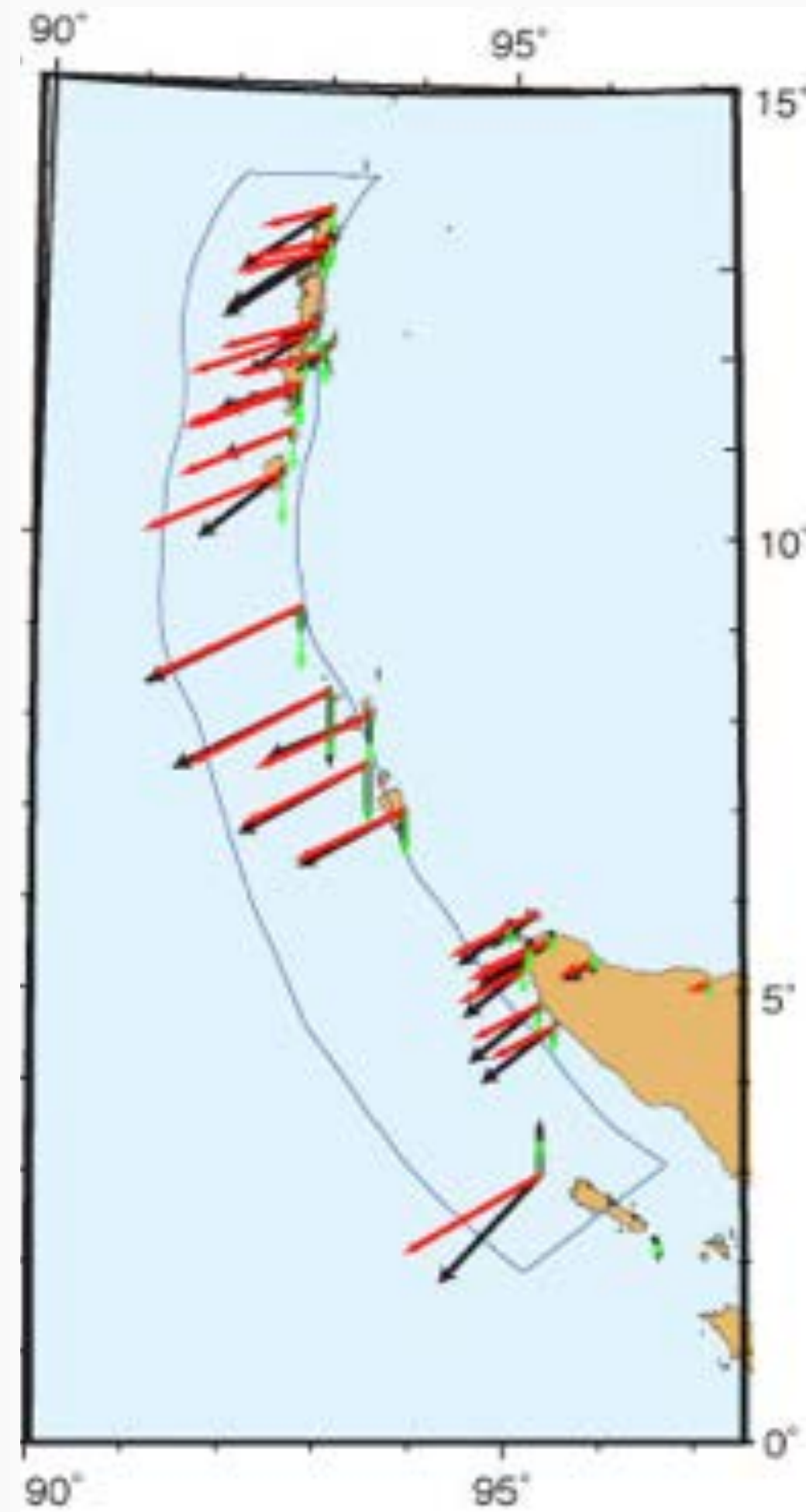
**Increasing  $P_f$ , decreasing effective normal traction**



Scenario 3  
Scenario 2  
Scenario 1

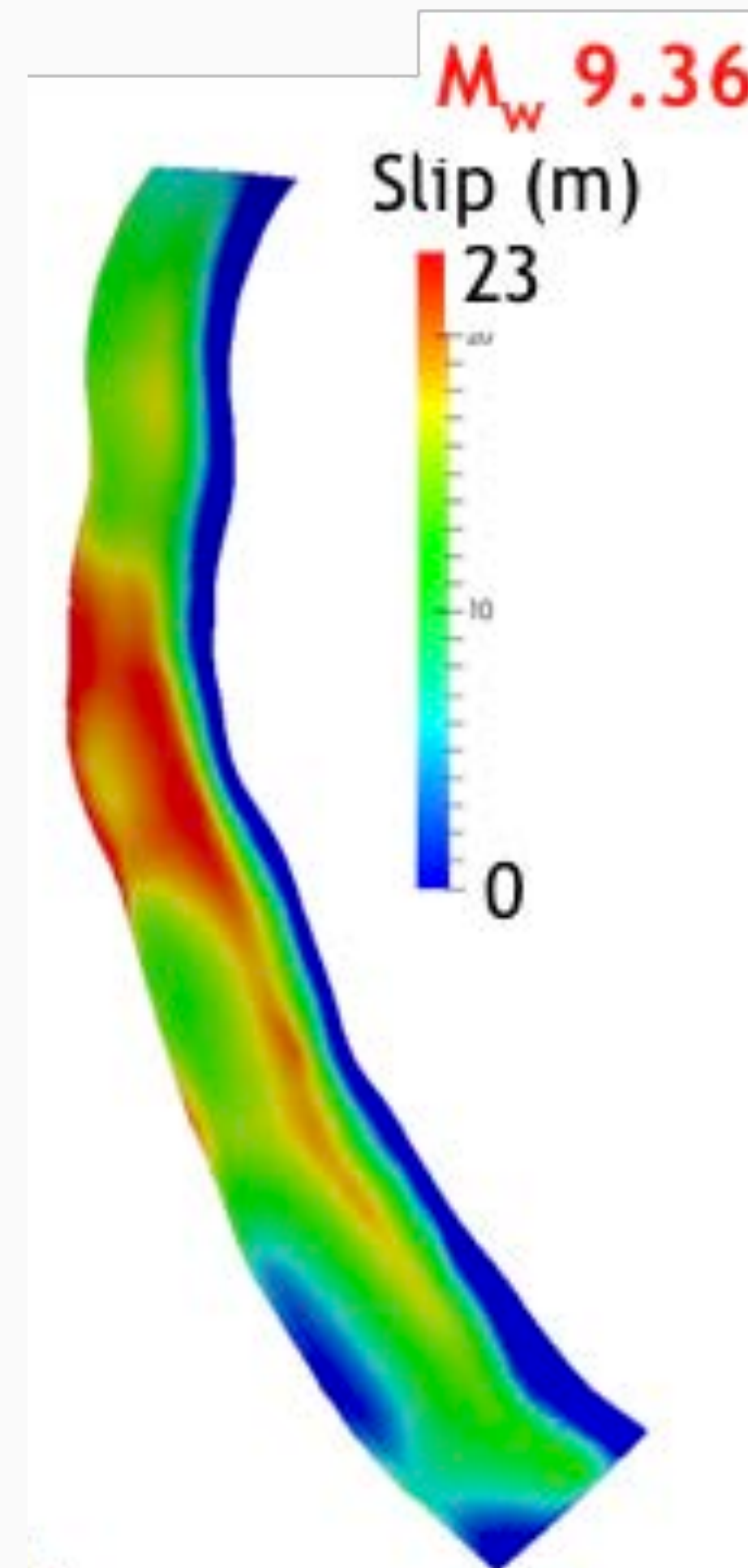


- The base model achieves reasonable:
  - earthquake magnitude;
  - estimated slip magnitudes;
  - GPS displacement orientations & magnitudes

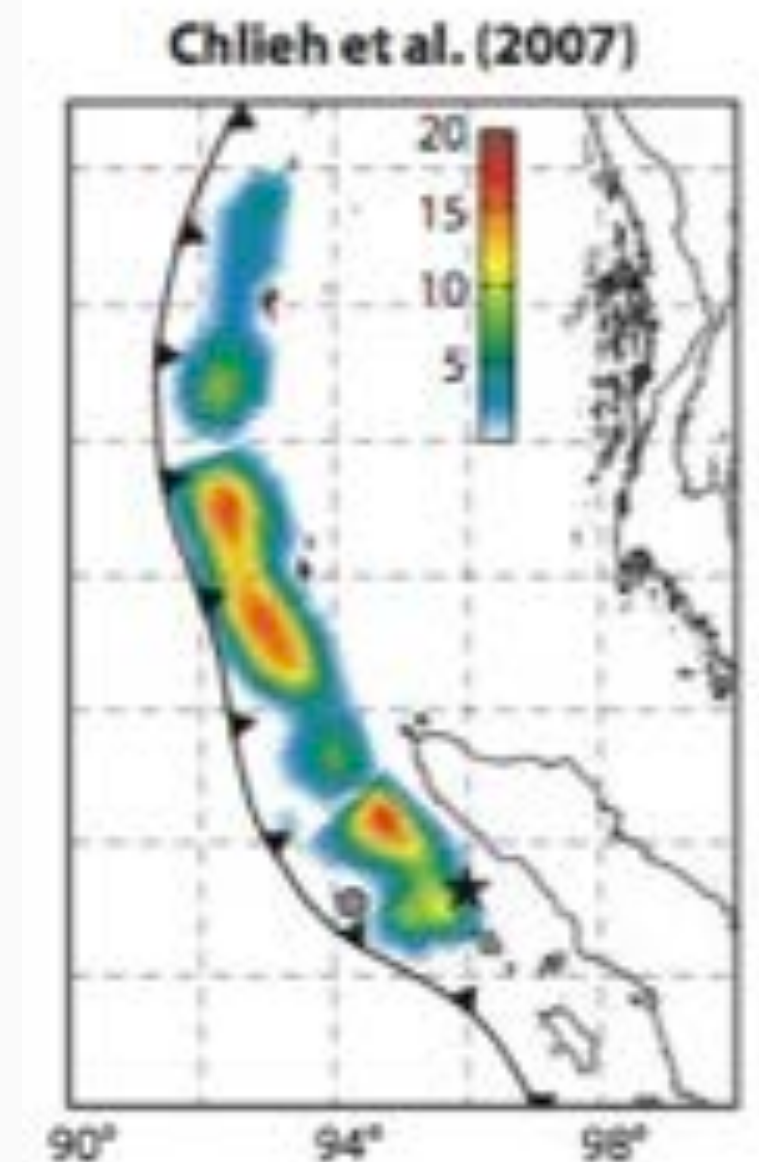
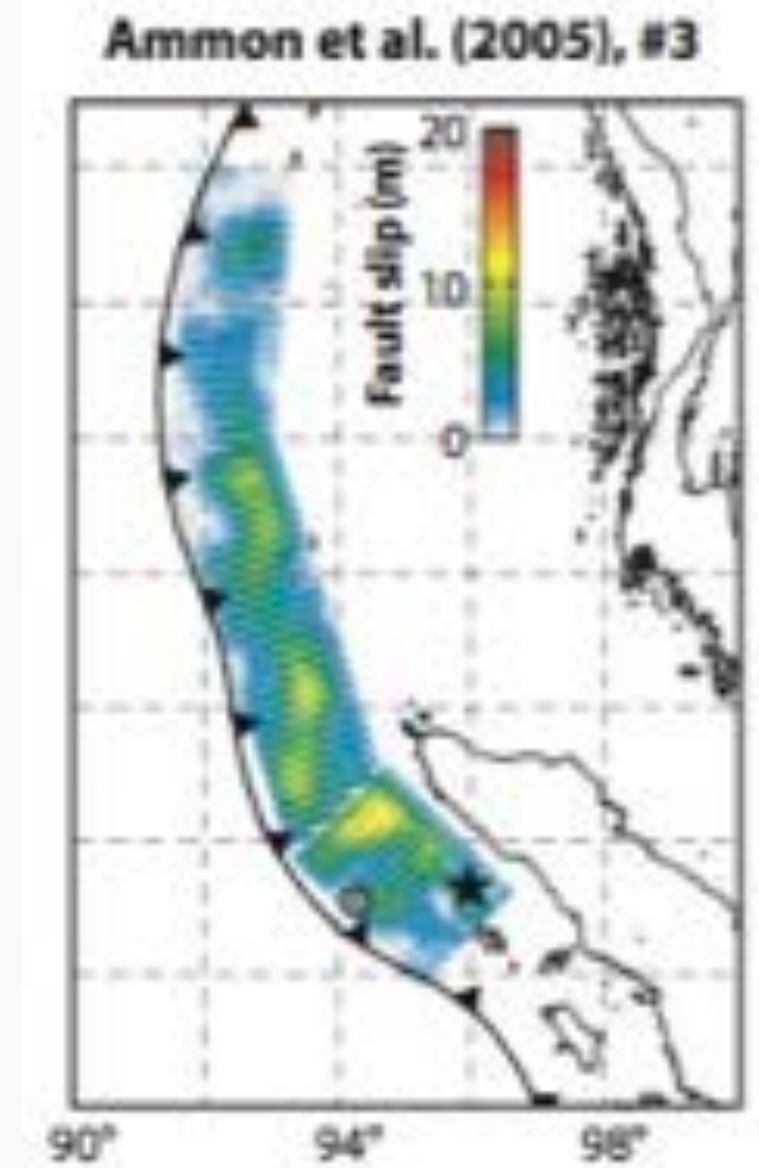


**Modeled (red and green) and observed (black) GPS displacements**

Data from: Subarya et al, 2006, Jade et al, 2005, Gahalaut et al, 2006



**Modeled slip distribution and moment magnitude**



**Slip distributions from kinematic source inversions (Shearer & Burgmann, 2010)**

We use the 2004 Sumatra earthquake as a test case to study the effects of pore fluid pressure (Pf) on megathrust mechanics & earthquake rupture dynamics.

We find that with depth-dependent stresses and depth-dependent Pf:

- shear and the normal tractions are both affected by Pf;
- the ratio of the shear to normal traction does not change with Pf.

Keeping friction constant across all models results in the following for models **with lithostatic Pf**, relative to hydrostatic Pf:

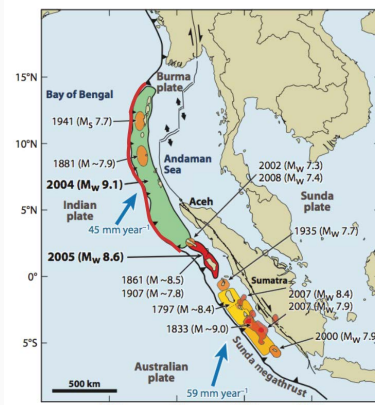
- lower shear strength;
- lower stress drop;
- less slip;
- lower earthquake magnitude;
- **slower rupture velocity;**
- **lower surface displacements;**
- similar slip patterns, except near the seafloor, where cohesion increases toward the surface.

We use the 2004 Sumatra earthquake as a test case to study the effects of pore fluid pressure (Pf) on megathrust mechanics & earthquake rupture dynamics. We find that with depth-dependent stresses and depth-dependent Pf:

- shear and the normal tractions are both affected by Pf;
- the ratio of the shear to normal traction does not change with Pf.

Keeping friction constant across all models results in the following for models with lithostatic relative to hydrostatic Pf:

- slower rupture velocity;
  - lower surface displacements;
  - lower shear strength;
  - lower stress drop;
  - less slip;
  - lower earthquake magnitude;
- where cohesion increases toward the surface.

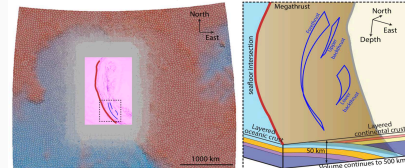


The 2004 Sumatra earthquake ruptured 1200 km of the Sunda megathrust (from Shearer & Burgmann, 2010).

**Starting model:** We produce a realistic 3D dynamic rupture model of the 2004 Sumatra earthquake with the following set-up. The value for Pf and the friction coefficients change in the 4 models presented below, but not the set-up or processes.

### Geometry & materials

- Slab geometry from Slab 1.0 (Hayes et al., 2012), with 3 splays
- Material properties from Crust 1.0 (Laske et al., 2013)

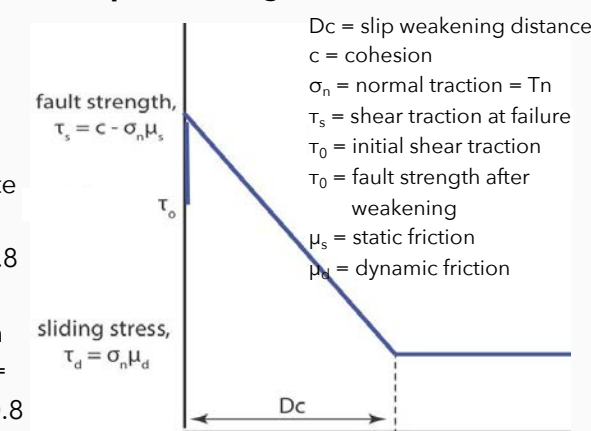


**Model set-up:** (left) Model domain and relative mesh sizes, (right) Splays and layered materials (Uphoff et al, 2017)

### Stress & fault strength

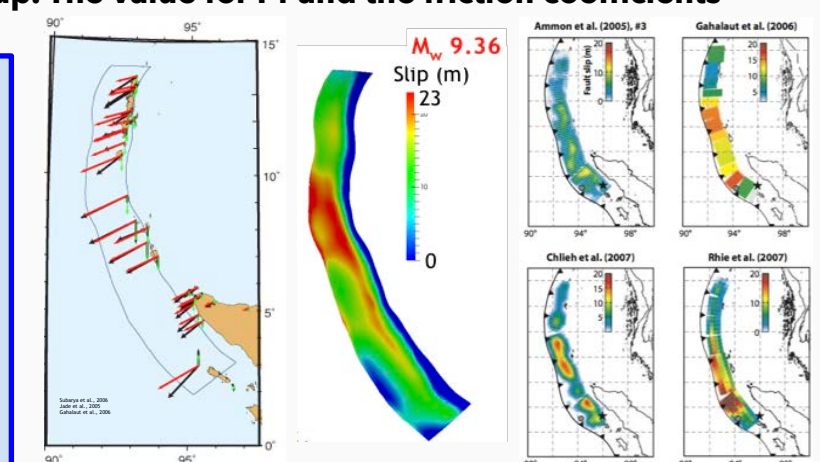
- Maximum compressive stress: azimuth = 225°, plunge = 7° (Karagianni et al., 2016)
- Depth-dependent absolute stresses
- Pf = -1800gz, where g = 9.8 m/s, z = depth
- Linear slip weakening with coefficients of friction:  $\mu_s = 0.15$ ,  $\mu_d = 0.82$  and  $D_c = 0.8$
- C = 0.4 MPa, increases to

### Slip-weakening friction law



Models are run with **SeisSol** ([www.seissol.org](http://www.seissol.org)), an open-source, 3D dynamic rupture & seismic wave propagation code optimized for high-performance computing (Uphoff et al., 2017)

- Using a low-resolution mesh with 4 mio cells, order 4 accuracy
- The model achieves:
  - Reasonable earthquake magnitude;
  - Estimated slip magnitudes;
  - GPS displacement orientations & magnitudes



**Model results:** (left) Surface displacements relative to observed, (right) Final slip magnitudes along the megathrust. **Slip distributions:** from kinematic source inversions (Shearer & Burgmann, 2010)

## Initial conditions:

- These models differ from the starting model in Pf,  $\mu_s$  and  $\mu_d$ .
- We vary the pore fluid pressure, Pf, from model to model.
- This leads to different effective stress magnitudes.
- This also leads to different differential stress magnitudes ( $S_{diff} = S1-S3$ ).
- Both the normal & shear stress are affected, as shown by Mohr circles that shift due to normal stress changes and change size with  $S_{diff}$ .
- As a result, both the shear and normal tractions along the non-planar megathrust change with Pf.
- The ratio of the shear to normal tractions does not change with Pf.
- Prestress ratio,  $R = (T_0 - T_s) / (T_d - T_s)$
- Relative strength parameter,  $S = (T_s - T_0) / (T_0 - T_d)$

## Earthquake characteristics:

- Stress drop controls rupture velocity and both are directly affected by Pf. Mean stress drop is estimated to be 3 MPa (Seno, 2017). Estimated rupture time is 480-600 seconds (Lal et al., 2005).
- Displacement & slip magnitudes are affected by Pf. Patterns are similar, except near seafloor due to cohesion.

